NASA CR-72398

MEASUREMENT OF THE CHARGE EXCHANGE CROSS SECTION OF MERCURY

by

DAVID ZUCCARO

CONTRACT NAS 3-7932

prepared for

NATIONAL AERONAUTICS AND SPACE ADMINISTRATION

HUGHES RESEARCH LABORATORIES
A DIVISION OF HUGHES AIRCRAFT COMPANY
3011 MALIBU CANYON ROAD
MALIBU, CALIFORNIA 90265

NASA CR-72398

FINAL REPORT

MEASUREMENT OF THE CHARGE EXCHANGE CROSS SECTION OF MERCURY

by

David Zuccaro

Prepared for

NATIONAL AERONAUTICS AND SPACE ADMINISTRATION

Submitted August 1967

Approved April 1968

CONTRACT NAS3-7932

Technical Management
NASA Lewis Research Center
Cleveland, Ohio

HUGHES RESEARCH LABORATORIES
3011 Malibu Canyon Road
Malibu, California

TABLE OF CONTENTS

LIST OF ILLUSTRATIONS

I. INTRODUCTION

This report covers the work performed by Hughes Research Laboratories for the Lewis Research Center of the National Aeronautics and Space Administration under Contract NAS 3-7932. This program was directed toward the experimental determination of the resonant charge exchange cross section of thermal velocity mercury atoms and singly charged mercury ions in the energy range 10^2 to 10^4 eV. The cesium ion and atom charge transfer cross section was also determined in the same apparatus as a verification of the mercury case.

Knowledge of the charge transfer cross section is of considerable importance in the design and evaluation of ion thrusters. Defocused ions are formed by charge transfer between ions and atoms in the ion beam. These charge exchange ions bombard the accelerator electrode, causing sputter erosion; this represents one of the most important factors limiting the operating life of the ion thrusters. The ion beam neutralizer is another vital component which is subject to sputter erosion. As a consequence, the charge exchange cross section must be known accurately for the design of the thrusters and the evaluation of their performance. In addition to this very practical application, knowledge of the resonant charge exchange cross section is essential to the development of a theoretical understanding of this process.

The experimental program was established to determine the mercury charge exchange cross section because of the uncertainty in previous experimental and theoretical values. These values are summarized in detail in Section II. The charge transfer cross section of cesium (the other ion propellant) has been determined by a number of investigators; based on the precise work of Marino[1,2] and Perel,[3] it is believed to be well established.

The experiment involved the use of an electron bombardment gas discharge ion source and a temperature controlled vapor source. The slow ions formed by charge transfer were removed from the reaction zone by a weak electric field normal to the ion beam axis. Details of the design and operation of the apparatus are presented in Section III.

The charge transfer ion currents were measured as functions of the ion beam energy, the gas density in the transfer region, the path length of the transfer region, and various ion source operating parameters. The mercury data fit a theoretical relationship* $\sigma^{1/2} \times 10^{8} = A - B \log V$ where σ is the cross section in cm^2 and V the ion energy in eV. A least squares fit of 1023 data points gave values of $A = 8.623$ and $B = 0.6354$. These values are significantly smaller than those of Paliukh and Sena,[4] and Badareu and Hagiescu.[5,6] The values are in close agreement with the theoretical values of Rapp and Francis.[7]

A small number of measurements of cesium charge exchange cross section were made to correlate this study to the previous cesium studies. Approximately 100 data points were obtained. The values obtained were slightly greater than those of Perel, et al.,[3] and were clustered about Marino's[1,2] values. Because of the large intervals in ion energy, no attempt was made to fit the data to expressions used by Marino[3] to describe the cross section.

*The theoretical relationship for $\sigma^{1/2}$ may be presented in terms of either ion energy or ion velocity v because the kinetic energy (expressed in eV) equals the kinetic energy (expressed as $1/2\, mv^2$, where m is the ion mass). We have chosen to express σ in terms of the ion energy because this is the directly measured parameter.

II. BACKGROUND

Resonant charge transfer is one of a number of reactions involving the inelastic collision of an ion and an atom of the same chemical species. These reactions are summarized briefly in Table I; this summary is based mainly on Hastead's work.[8] In the table, the subscripts 1 and 2 identify the specific atomic particle M. The superscripts o, +, and * indicate a neutral, an ionized, and an electronically excited state of the particle. The numerical subscripts (0, 1, 2) used in the reaction cross section notation refer to the neutral atom and the single and double charged ion. The subscripts preceding σ represent the initial state of the system, and those following represent the reaction products.

TABLE I

Summary of Reactions

	Reaction		Cross Section Notation
1.	$M_1^+ + M_2^o \rightarrow M_1^+ + (M_2^o)^*$	Excitation	$10^{\sigma}10^*$
2.	$M_1^+ + M_2^o \rightarrow M_1^o + M_2^+$	Charge exchange	$10^{\sigma}01$
3.	$M_1^+ + M_2^o \rightarrow M_1^o + (M_2^+)^*$	Charge exchange with excitation	$10^{\sigma}01^*$
4.	$M_1^+ + M_2^o \rightarrow M_1^+ + M_2^+ + \text{electron}$	Ionization	$10^{\sigma}11$
5.	$M_1^+ + M_2^o \rightarrow M_1^{++} + M_2^o + \text{electron}$	Stripping	$10^{\sigma}20$

In this program we are concerned with the cases where M_1^+ represents a fast ion (i.e., one with energy much greater than thermal energy) and M_2^o represents a thermal atom.

Those inelastic collisions characterized by reaction 1 may have a significant cross section; but because there is neither the production of thermal velocity ions nor attenuation of the primary ion current (M_1^+), this reaction will be ignored in this discussion. The electron stripping reaction (No. 5) occurs at ion energies greater than the maximum energy used in this experiment, and therefore is not significant in this experiment.

The ionization reaction (No. 4) is not observed at low beam energies; although it is observed for ions in the energy range of 5 to 10×10^3 eV, its cross section ($_{10}\sigma_{11}$) is small compared with $_{10}\sigma_{01}$ in this energy range. However, this reaction can have a pronounced effect in charge exchange measurements and thus must be considered. As a result of the reaction, a slow ion (M_2^+) is formed which could be mistakenly interpreted as an ion formed by charge exchange. An error also results because the fast ion current (M_1^+) is not attenuated. Failure to account for the ionization reaction causes the apparent $_{10}\sigma_{01}$ value to be too large. The magnitude of reaction 4 is determined by measuring the free electron current. This method of distinguishing between reactions 4 and 2 is discussed in more detail in Section IV.

The charge transfer processes (reactions 2 and 3) involve the transfer of an electron from the atom (M_2^o) to the ion (M_1^+) during the period when these two species are within a finite internuclear separation. Because there is only transfer of an electron (whose mass is negligible compared with the atomic mass M), the process is essentially inelastic. This means that there is no transfer of momentum between the two particles, and they retain their original kinetic energies. Thus the fast ion (M_1^+) becomes a fast neutral (M_1^o) with no change in the direction of travel. The gas (M_2^o) which has thermal energy is converted into an ion (M_2^+) which has the kinetic energy of the original gas (M_2^o). Both theoretical analysis and experimental results have shown that the cross section $_{10}\sigma_{01}$ increases as the interaction time increases (or conversely as the relative velocity of the ion with respect to the atom decreases). The value of $_{10}\sigma_{01}$ is greatest for the lowest energy ions.

In addition, for a given relative velocity, $_{10}\sigma_{01}$ increases as the ionization potential decreases. The maximum cross section should be observed for low energy ions of low ionization potential.

There is no electronic difference between charge exchange to ground states (reaction 2) and charge exchange with excitation (reaction 3). The difference is significant in the theoretical calculation of the cross section.

A. Theoretical

Massey and Smith[9] performed a quantum mechanical calculation of resonant charge exchange using the method of perturbations of the electronic wave junctions. The study was limited to the interaction of helium atoms and 1000 eV helium ions. Firsov[10] and Smirnov[11, 12] derived a relationship which had the form $\sigma = (\pi R_o^2/2)$ where R_o is an impact parameter dependent on a term $(\epsilon_u - \epsilon_g)$ (which represents the splitting of the atomic electron energy levels when the ion approaches the atom and on the internuclear distance R). Firsov's theoretical value for the mercury charge exchange cross section is shown in Fig. 1.

Demkov[13] derived an expression for the charge transfer cross sections of atom hydrogen and of helium. He generalized it to the following expression for any monoatomic gas with one valence electron:

$$\sigma^* = \frac{1}{I}\left[48 - \log\frac{V}{M}\right]^2 (a_o)^2 \qquad (1)$$

where I is the ionization potential in eV, V the ion energy in eV, M the atomic weight, and σ^* is the cross section expressed in terms of Bohr radii. A conversion factor of 0.28×10^{-16} is used to put σ in units of square centimeters.

$$\sigma = \frac{1}{I}\left[48 - \log\frac{V}{M}\right]^2 \times 0.28 \times 10^{-16}\ \text{cm}^2 \qquad (2)$$

This expression has been evaluated for the mercury cross section and the result is plotted in Fig. 1.

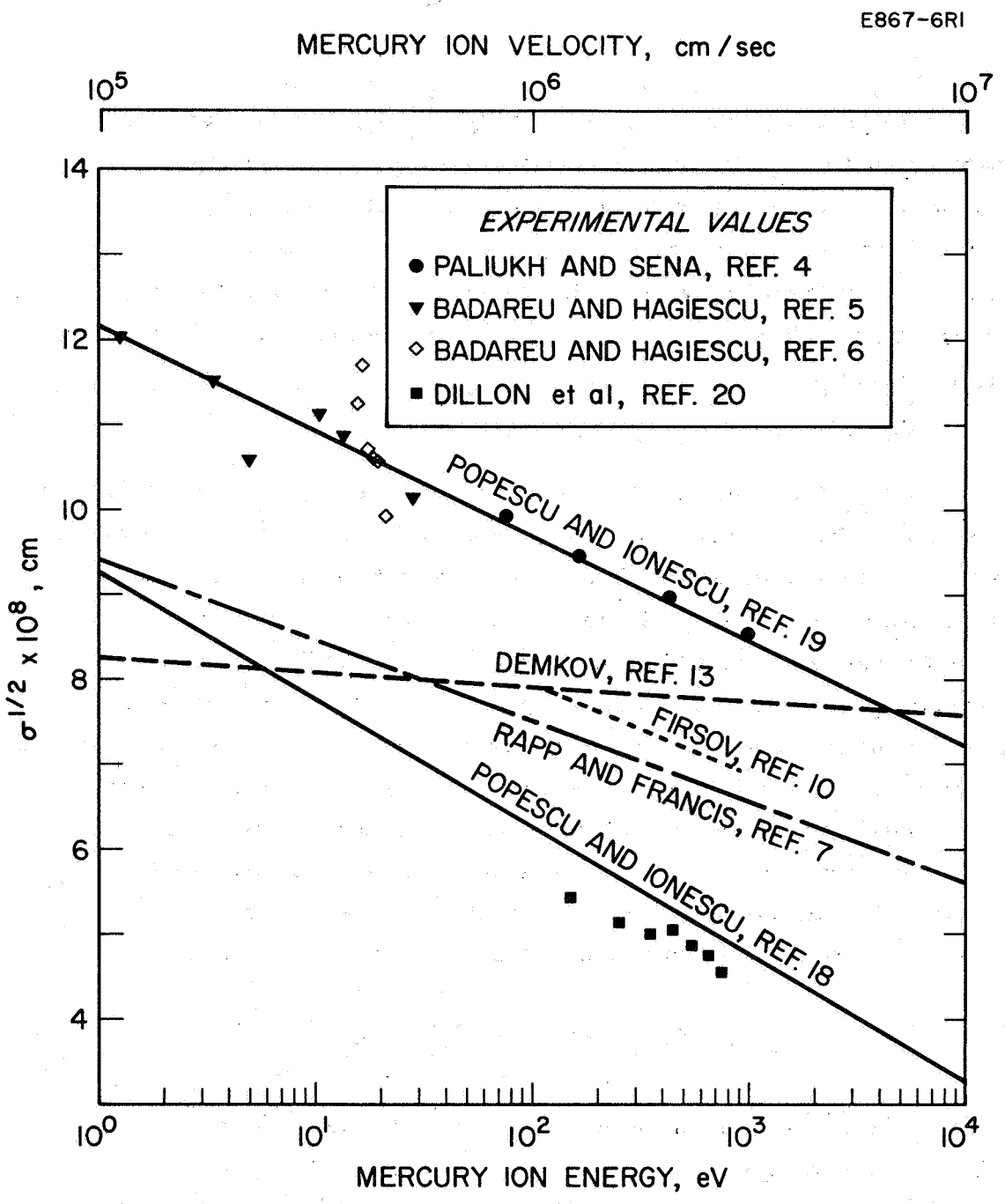

Fig. 1. Previous experimental and theoretical values of the mercury charge exchange cross sections.

Rapp and Francis[7] developed a complex expression for σ which depends on an impact parameter b which is a function of the energy states of the electron and ion, on the velocity of the ion v, and on the ionization potential of the atom. The cross section was given as

$$\sigma = \frac{\pi}{2} b_1 \tag{3}$$

where b_1 is an approximate value of b. The value of b_1 is obtained by solving (4) for b_1 at a specific value of v:

$$\left[\left(\frac{2\pi}{\gamma a_o}\right)^{1/2}\left(\frac{I}{\hbar v}\right) b_i^{3/2}\left(1 + \frac{a_o}{\gamma b_1}\right) \exp\left(- \frac{\gamma b_1}{a_o}\right)\right] = \frac{\pi}{6} \tag{4}$$

in which $\gamma = (I/13.6)^{1/2}$, a_o is the radius of the first Bohr orbit, and $\hbar$ is Planck's constant divided by 2π. The cross section is then obtained using $\overline{b_1}$, which is an average value of b_1 obtained from (4).

$$\sigma^{1/2} = - \left(\frac{\pi}{2}\right)^{1/2}\left(\frac{a_o}{\gamma}\right) \ln v + \left(\frac{\pi}{2}\right)^{1/2}\left(\frac{a_o}{2\gamma}\right) \ln\left[\frac{72\,\overline{b_1}^3}{\pi\gamma\, a_o}\left(\frac{I^2}{\hbar^2}\right)\left(1 + \frac{a_o}{\gamma \overline{b_1}}\right)^2\right] \tag{5}$$

Equation (5) has the form $\sigma^{1/2} = - k_1 \ln v + k_2$. Their theoretical value for mercury is shown in Fig. 1. Their derivation was limited to symmetrical state reactions (No. 2 of Table I). They did not consider excitation reaction No. 3 of Table I, which may have a significant cross section.

Smith[14] has used a two state wave theory with two potentials whose difference passes through a maximum to obtain the expression which exhibits the oscillation in ${}_{10}\sigma_{01}$ as a function of the relative ion velocity observed by Perel[3] and Marino[2] in the cesium charge exchange cross section.

The theoretical values obtained by Popescu-Iovitsu and Ionescu-Pallas will be considered in the next section.

B. Experimental

The mercury charge exchange was first measured by Paliukh and Sena.[4] Their apparatus (shown in Fig. 2) consisted of a glass tube in which the ion source consisted of a mercury vapor discharge maintained between a mercury pool cathode P_1 and several anodes (A_1, A_2, A_3, A_4, and D). A fraction of the ion current to the molybdenum anode D traveled through a 4 mm screened hole in the anode into a region behind it. The ions passed through a 10 mm diameter screen S_1 which was located 2 mm from D. They then traveled a distance L to a second nickel screen S_2 which was located 1.3 mm from an iron collector K. A potential on S_1 gave the ions the required energy. Charge exchange occurred in the region between S_1 and S_2 which was varied for L of 10 to 43 mm. The entire unit was placed in a constant temperature bath to establish the mercury vapor pressure.

The measurements were made using modifications of the retarding field method. In one case, the potential on K and S_2 was common. In a second case, S_1 and S_2 were at a constant potential difference. The third case had a constant potential on S_1 and K. Paliukh and Sena determined the ratio of I_o/I (where I_o is the ion current entering the collision region and I is the attenuated current) by measuring the collector current as a function of the potential which was varied. These data were obtained as a function of path length and mercury temperature (i.e., vapor pressure). The vapor pressure was obtained from Mayer's[15] relationship, $\log P = 10.5724 - 0.847 \log T - 3342.26/T$ where P is in Torr and T in ^{o}K.

The data were taken for mercury ions in the energy range of 32 to 1400 eV. The cross section for charge transfer was determined at four energy values for which the most complete data were obtained. These are plotted in Fig. 1, and summarized in Table II where Q is the cross section expressed in terms of the gas density at $273.2^{o}K$ and σ the cross section which is expressed in square centimeters. These same data are presented in a more recent paper by Kushnir, Paliukh, and Sena.[16]

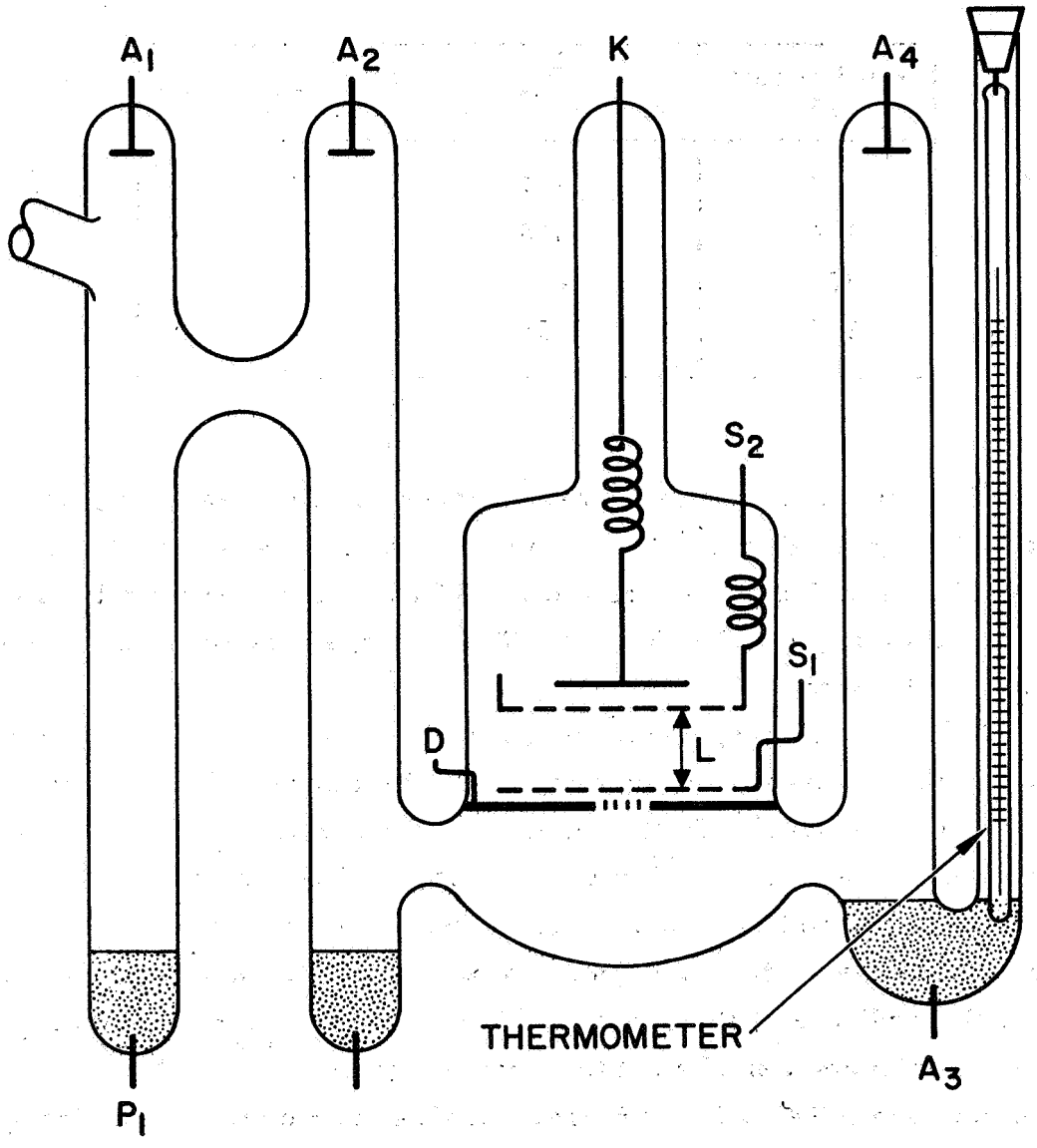

Fig. 2. Schematic view of apparatus used by Paluikh and Sena (Ref. 4).

TABLE II

Mercury Charge Exchange Cross Section (Ref. 4)

Ion Energy, eV	Q, cm^2/cm^3 Torr	σ, $cm^2 \times 10^{16}$
75	351	98.7
165	316	88.8
425	286	80.4
990	258	72.5

The mercury charge exchange cross section was also measured by Badareu and Hagiescu[5-6] by means of a simple retarding field method of measuring low energy ion mobilities in a mercury discharge; their results are plotted in Fig. 1. These same data were also summarized by Popescu.[17]

Some uncertainty concerning the probable value of the mercury charge exchange cross section has resulted from the 1959 publication of Popescu and Ionescu.[18] In this paper they developed a theoretical expression of the form $\sigma^{1/2} = k_1 - k_2 \log v$. Their graph of this expression appeared to be a very close fit to the data of Refs. 4, 5, and 6. Unfortunately, this is not found to be true. Although the authors labeled the ordinate of the graph $\sigma^{1/2} \pi^{1/2} \times 10^{-8}$, they plotted the data of Paliukh and Sena[4] as if the ordinate were $\sigma^{1/2} \times 10^{-8}$. The plot of data from Refs. 5 and 6 does not fit either choice of ordinate. In addition, the values of the constants k_1 and k_2 given in a table and plotted on the graph do not agree with the values obtained from the expression given for these constants.

In 1960, the same authors[19] published a seemingly identical derivation which produced a new set of values for k_1 and k_2. Although these constants produce values of σ that are in close agreement with the previous experimental values (see Fig. 1), it is not possible to obtain the values of k_1 and k_2 from the derived expressions. The

authors do not explain the difference between these two publications. Because of the ambiguity that exists, these theoretical values will not be considered in this study.

Dillon, et al.,[20] measured the charge transfer of mercury and a number of other gases using a beam attenuation apparatus. Because of the uncertainty in determining the magnitude of the ion currents, they chose to standardize the apparatus by equating their 450 eV argon data to those of Hastead.[21] This indirect method of calibrating the apparatus may be partially responsible for the fact that the mercury values obtained for 150 to 750 eV ions were much smaller than previous experimental values (Fig. 1).

C. Cesium Charge Exchange — Experimental and Theoretical Values

Of the eight experimental determinations of the cesium charge exchange cross section, the four most recent ones are in reasonably close agreement, implying that the value is fairly well established. The results of the first six experimental and two theoretical evaluations of the cross section are presented in Ref. 1. The results of Marino, et al., and of Chkuaseli, et al., (see Ref. 1) are in very close agreement, while the four other works are significantly smaller. Marino, et al.,[1] found the theoretical values of Rapp and Francis and of Firsov to be much smaller than the experimental values. Marino's[1] experiment involved the attenuation of a cesium ion beam by means of a temperature controlled cesium gas source. By means of least squares, he fitted 52 data points to the expression

$$\sigma^{1/2} \times 10^{8} = 26.8 - 1.46 \ln V$$

$$= 26.8 - 3.36 \log V$$

Perel, et al.,[3] obtained the cross section by attenuating an ion beam with a chopped atomic beam. They observed three peaks in the cross section which had not been reported previously. The expression

($\sigma^{1/2} \times 10^8 = a - b \ln v$) was evaluated for the combined cesium ion — cesium atom cross section data and rubidium ion-rubidium atom cross section data, and values of $a = 42$ and $b = 1.85$ are given. Analysis of the graph of the cesium data indicates that this combined expression gives an erroneously low value for σ. Based on the data obtained from the graph in this paper, an approximate value of the cross section is given by $\sigma^{1/2} \times 10^8 = 21.33 - 2.17 \log V$.

The oscillations in the resonant charge exchange cross section were analyzed by Smith[14] and explained using a two state wave theory in which the difference between the gerade and ungerade potentials passes through a maximum. Marino[2] remeasured the charge exchange for 10 V increments in ion energy and found five more peaks in the cross section. He developed a theoretical expression

$$\sigma = \sigma_o - A_1 V^{1/4} \cos \left[\pi(|B| V^{-1/2} - \tfrac{1}{4})\right] \qquad (6)$$

in which σ_o is the nonoscillating portion of the cross section, and $A = 0.75 \times 10^{-16}$ cm $(eV)^{-1/4}$ and $B = -820\ (eV)^{1/2}$ for the cesium case.

III. EXPERIMENTAL

A. Apparatus

The charge exchange apparatus consists of an electron bombardment ion source which forms a collimated ion beam that is directed through a temperature regulated neutral gas source. Inelastic (charge transfer) collisions occur between the ions and the gas, resulting in the formation of fast neutrals and slow ions. The slow ions are collected by a weak electric field which is perpendicular to the ion beam axis. This field is sufficient to collect the charge transfer ions, but it does not perturb the primary (energetic) ion beam. The charge exchange ion current is measured as a function of the neutral gas density, interaction path length, and primary ion beam energy. The measurements are made in an all metal ion pumped UHV chamber.

The mercury and cesium ions are produced in a magnetically confined low voltage electron bombardment ion source, which is shown in Fig. 3. The source consists of a hairpin-shaped tantalum cathode mounted along the axis of a 1.2 cm radius cylindrical anode. This in turn is surrounded by a solenoid which produces an axial magnetic field. The source is shown in schematic form in Fig. 4. The gas is ionized by electrons confined in a radial and axial potential well by the electric and magnetic fields. Vapor flow into the source is controlled by temperature regulation of an external reservoir. Typically, the source operated with a 40 V anode potential for mercury and 12 V for cesium, a discharge current of 50 to 100 mA, and a 50 to 70 gauss magnetic field. The electrical layout is shown in Fig. 5.

The ions were extracted through the screen electrode which had a 100 wire/cm, 58% transparent, 0.0013 cm thick molybdenum mesh placed over the 0.254 cm diameter orifice. The screen establishes the plasma boundary in the electrode and thus fixes the ion trajectories. This is essential because operation at low plasma densities without a screen could result in the formation of a plasma meniscus well inside the source,

M 5217

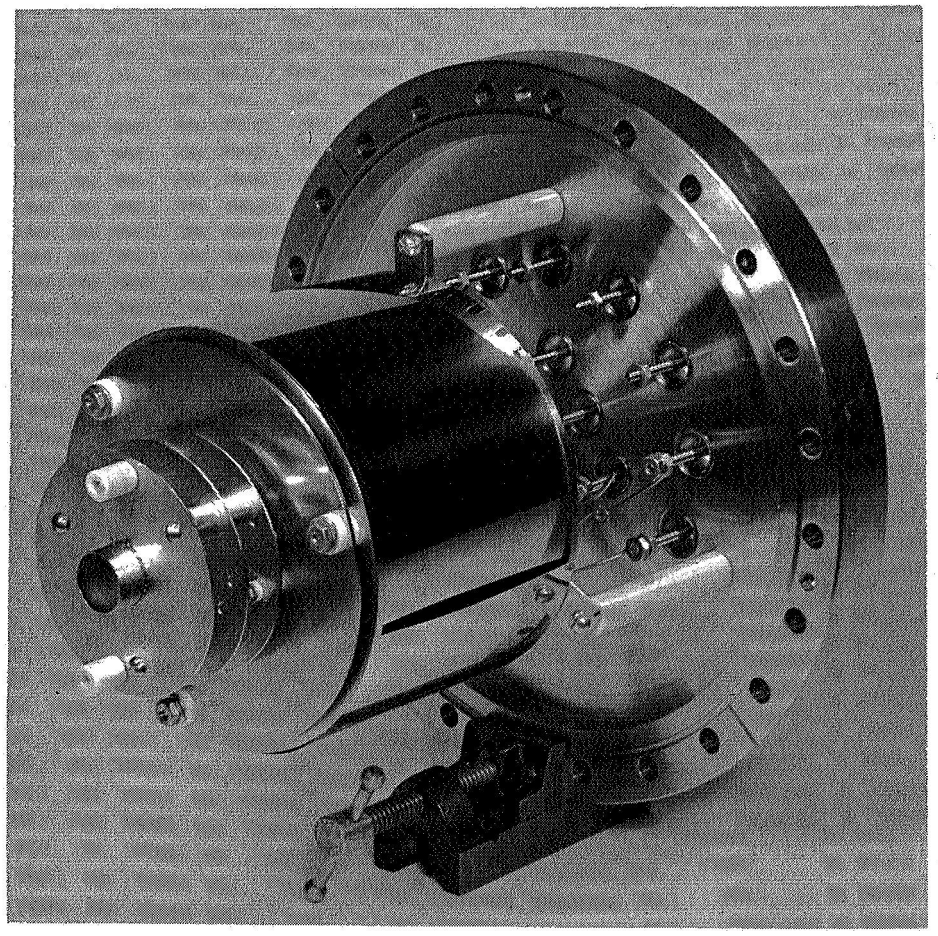

Fig. 3(a). Ion source, front view.

M 5218

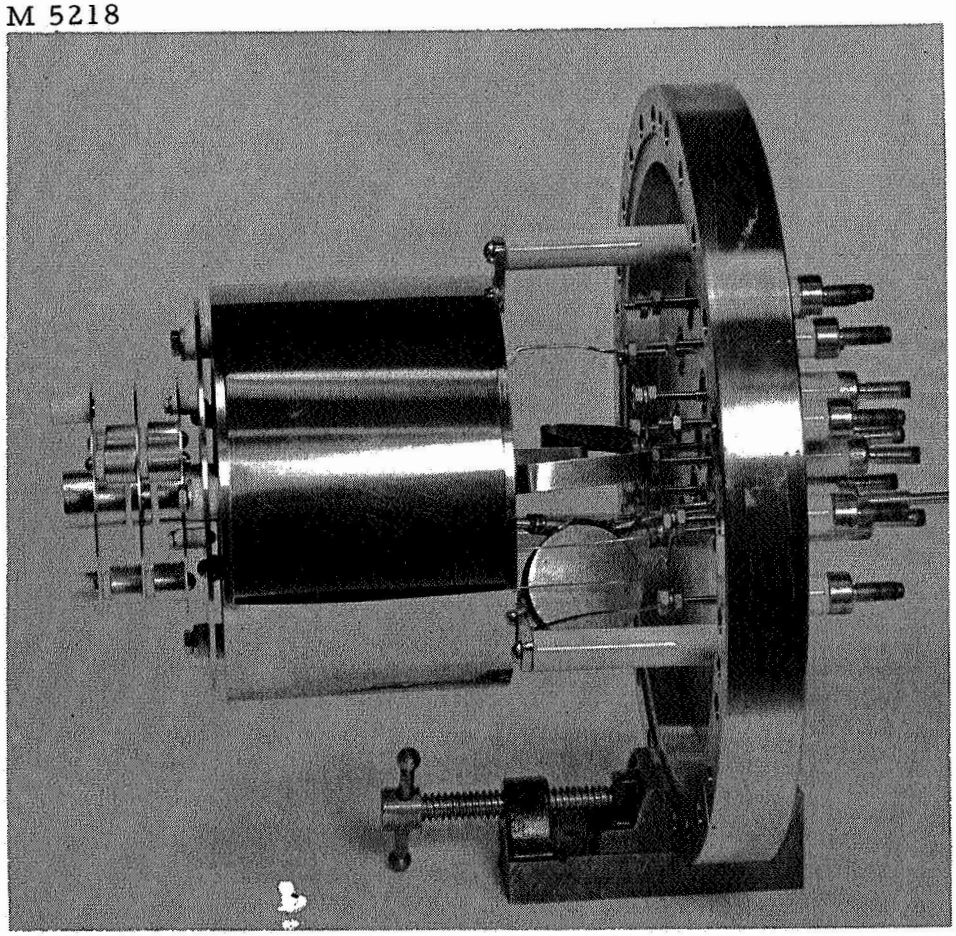

Fig. 3(b). Ion source, side view.

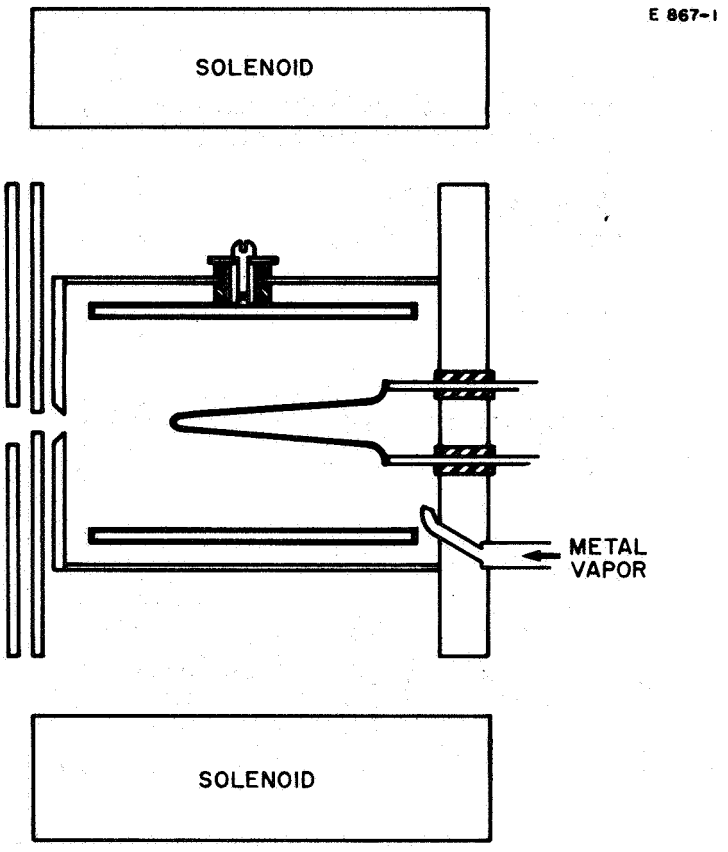

Fig. 4. Cutaway view of the ion source.

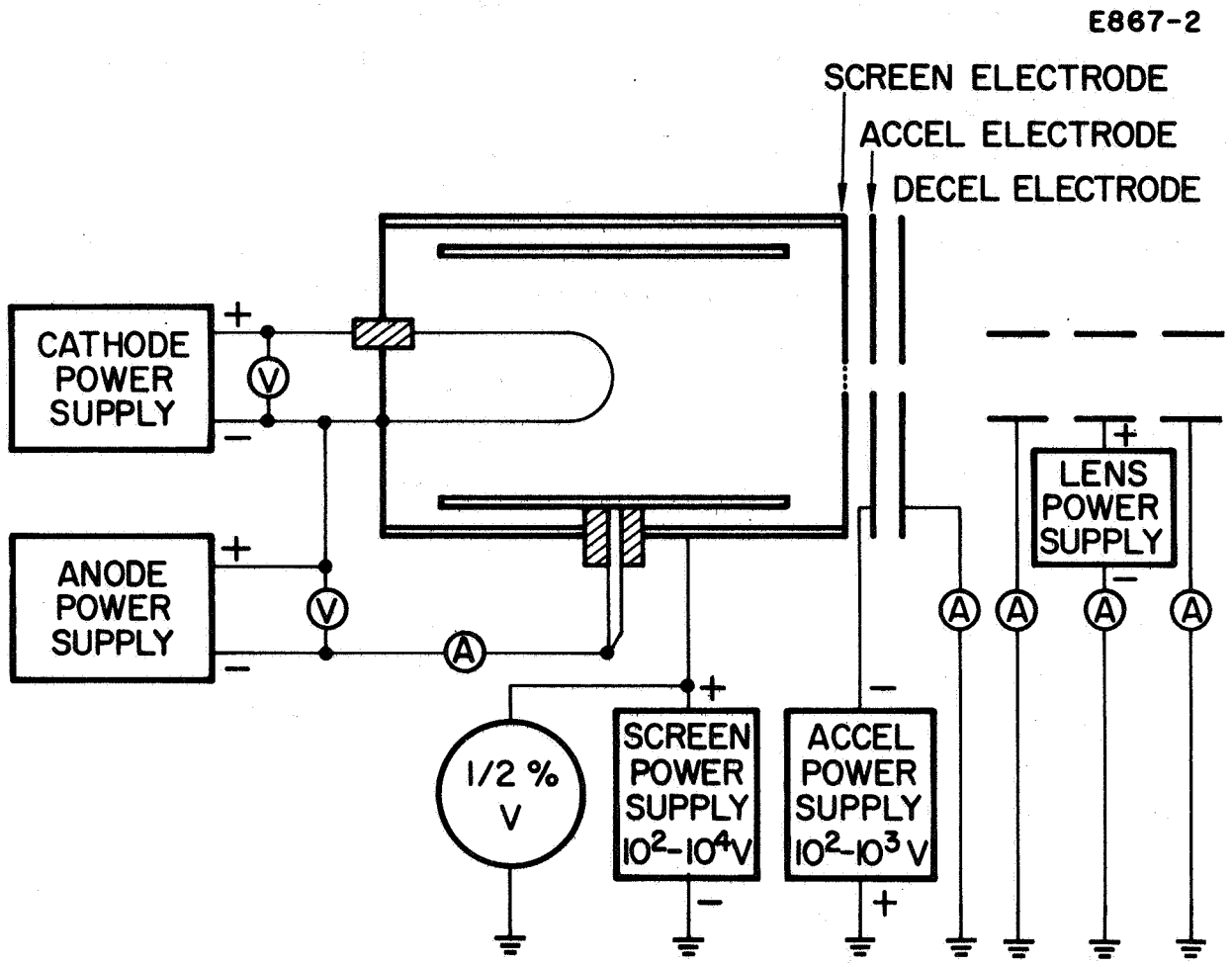

Fig. 5. Schematic representation of the electrical circuits of the ion source.

causing poor focus of the ion beam. The mesh size was determined by calculating the minimum plasma sheath thickness from the Langmuir-Child space charge equation on the basis of a 40 V discharge and an ion current density of 10 mA/cm^2.

The geometry of the source electrodes was determined by an electrolytic tank analog computer study in order to obtain maximum linearity of the ion trajectories over a wide range of electrode potentials. The electrode geometry is shown in Fig. 6 and the trajectory plots are shown in Fig. 7.

A three-element einsel (unipotential) electrostatic lens was fabricated, tested, and mounted on the ion source. It was to have been used if spreading of the ion beam occurred, causing the ion current in the charge transfer region to be too small for accurate measurement. This condition was not experienced during the entire experiment, so all elements of the lens were held at ground potential throughout the run.

The charge exchange measurements were made with a parallel plate diode enclosed in a chamber in which the gas density was temperature regulated. This is shown in cross sectional view of Fig. 8 and in complete detail in Figs. 9 and 10. This unit is positioned about 25 cm from the ion source. The unit functions in the following manner. The ion beam is monitored and collimated by the three electrically isolated shields. A bellows-sealed, manually operated shutter (located between the last shield and the chamber) turns off the beam prior to each measurement so that the background currents may be checked.

The chamber is fabricated in the form of two half cylinders. The lower half has a double wall through which an ethyl alcohol-glycol-water mixture is circulated from an external constant temperature bath. This bath is temperature regulated to $\pm 0.02^{\circ}K$, has a 13 liter fluid capacity, and circulates fluid to the lower half of the charge exchange chamber at a rate of 10 liter/min. A chromel-alumel thermocouple, spot welded to the interior of the chamber, was used to determine the temperature of the source of the neutral vapor. The junction potential was measured,

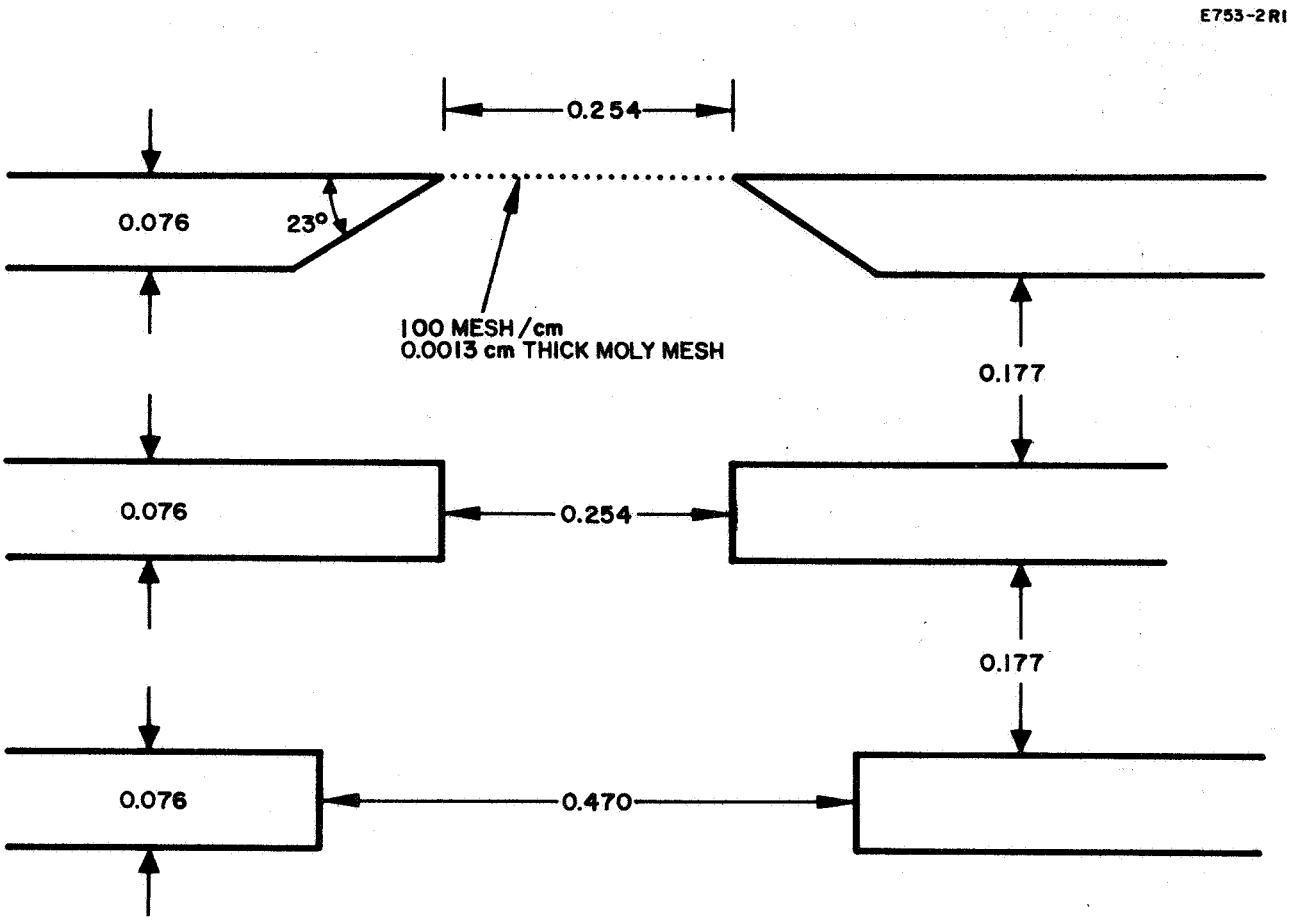

Fig. 6. Cross section of ion source electrodes as developed from electrolytic tank studies.

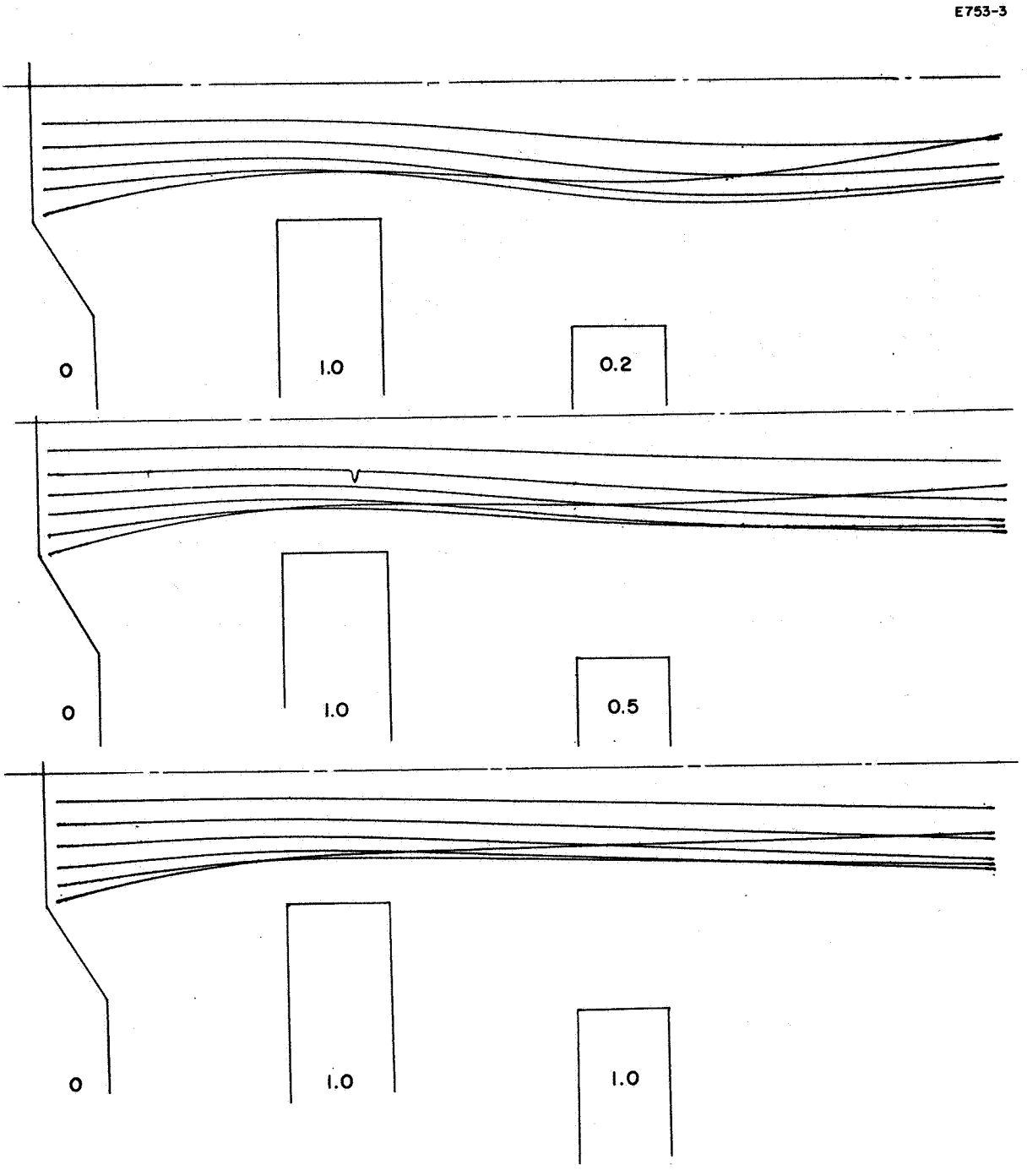

Fig. 7. Trajectory plots at various accel-decel potentials.

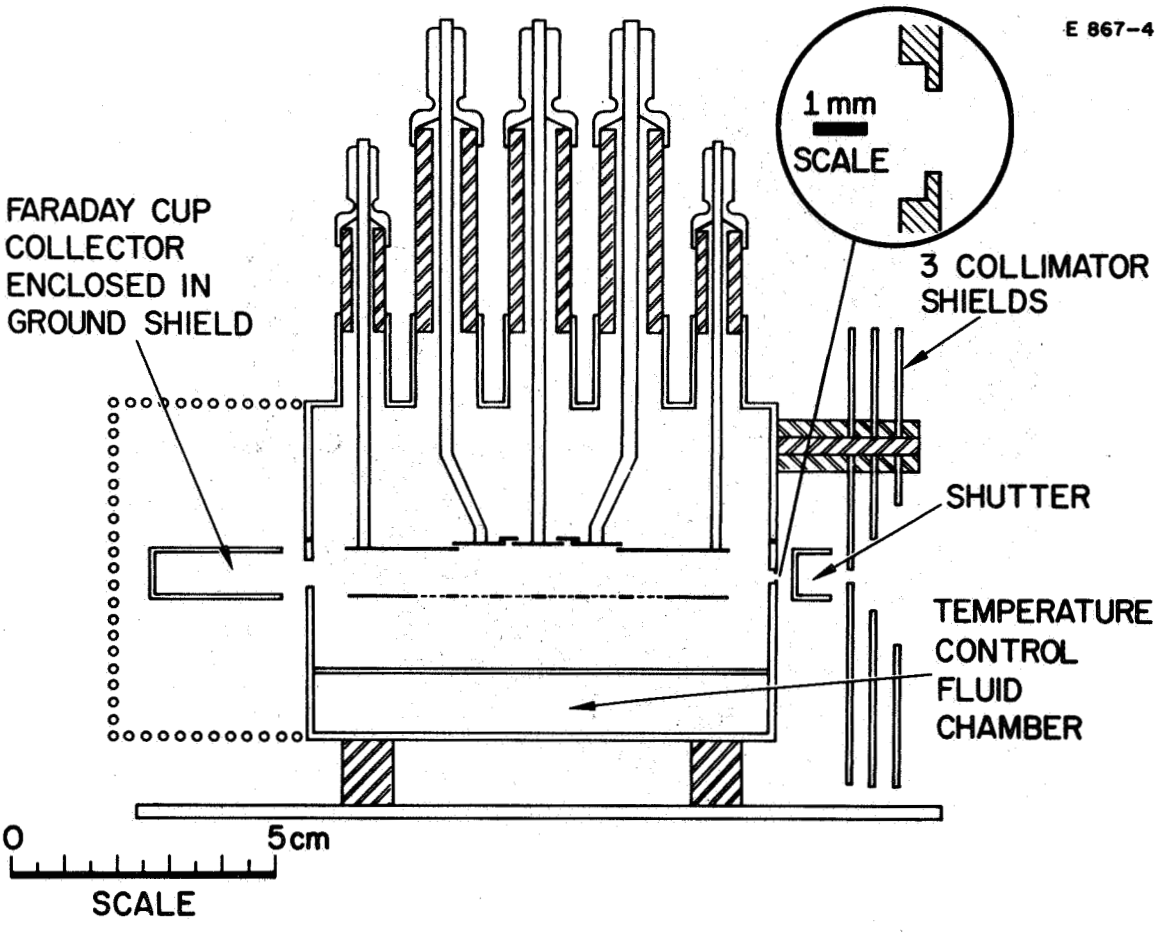

Fig. 8. Cutaway view of charge exchange chamber.

M 5251

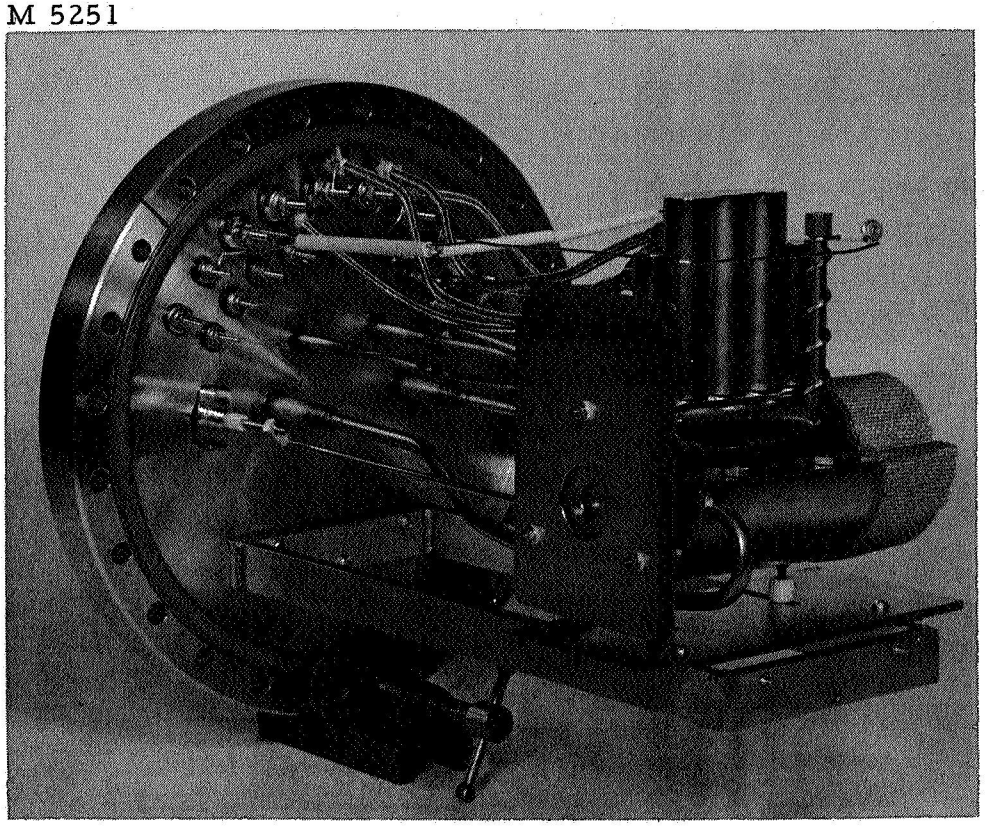

Fig. 9. Charge exchange chamber — view of end through which ion beam enters chamber.

M 5250

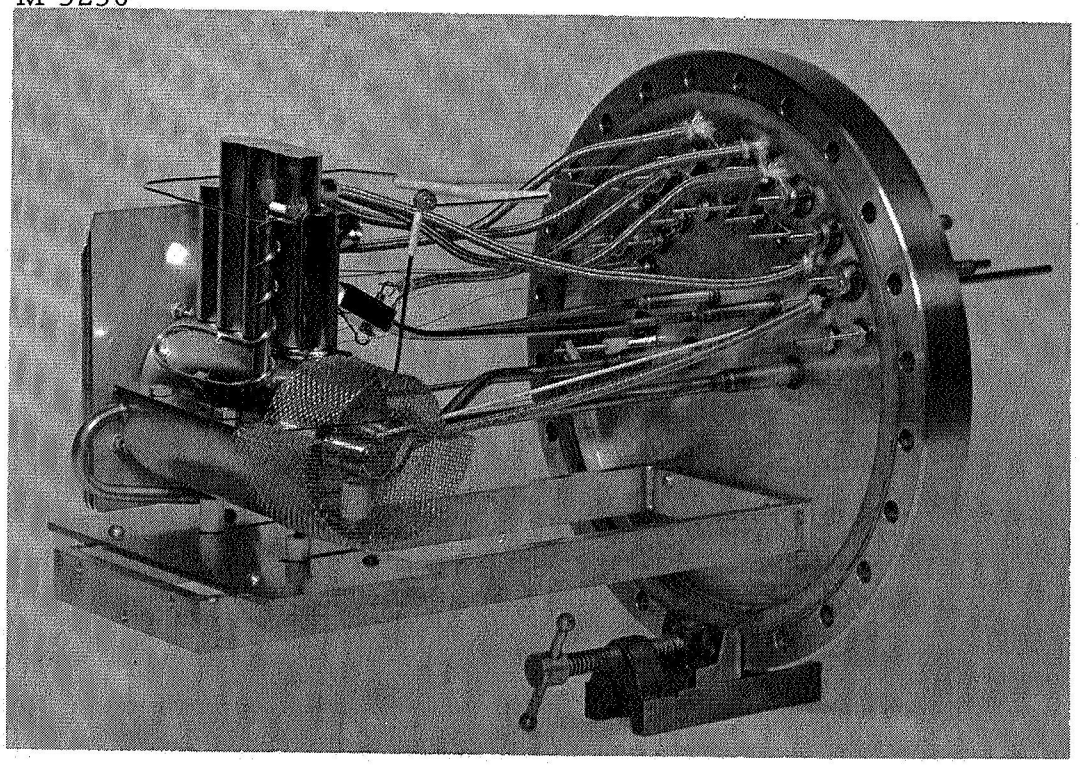

Fig. 10. Charge exchange chamber — view of end having Faraday collector.

with respect to an external reference junction located in a deionized water-deionized ice bath, by a potentiometer bridge of 0.001 mV sensitivity. In operation, the temperature of the metal vapor source was constant to within $\pm 0.03^{\circ}K$.

The upper half of the chamber is heated to approximately 50 to $75^{\circ}K$ higher than the vapor source by means of the stainless steel sheath heaters. This insures the vapor density regulation by the lower portion of the chamber.

The lower electrode of the diode is mounted in the lower half of the chamber on alumina rods and is positioned 0.381 cm below the ion beam axis. This 3.00 x 7.00 cm electrode (shown in Fig. 11) is ventilated to permit maximum communication of the vapor in the charge transfer region with the temperature controlled vapor source. A 97% transparent, 8 mesh/cm electroformed nickel mesh covers the holes in the electrode and establishes a uniform field.

The upper electrode consists of a 3.00 x 7.00 cm guard electrode (which has a 3.000 ± 0.003 by 1.000 ± 0.003 cm rectangular slot in it) and three collector electrodes each 1.000 ± 0.003 cm wide. These electrodes, which are suspended from cable end seals welded to the upper half of the chamber, are positioned 0.381 cm above the ion beam axis. Triaxial cable (stainless steel shields over quartz wool insulation) was used to carry the ion current signals to the vacuum headers.

The attenuated ion beam leaves the chamber and is measured by a 0.8 cm inside diameter, 2.54 cm long Faraday cup collector which is attached after the chamber is optically aligned to the source. A nickel ground screen surrounds the Faraday collector to prevent interference from stray ions or electrons.

The experiments were conducted in a stainless steel vacuum chamber 14 in. diameter and 42 in. long (see Figs. 12 and 13). This UHV facility includes a flooded liquid nitrogen cryoliner (12 in. diameter, 20 in. long) which is kept filled throughout the run. The system is pumped with 500 liter/sec ion pump and uses zeolite sorption pumps.

M 5249

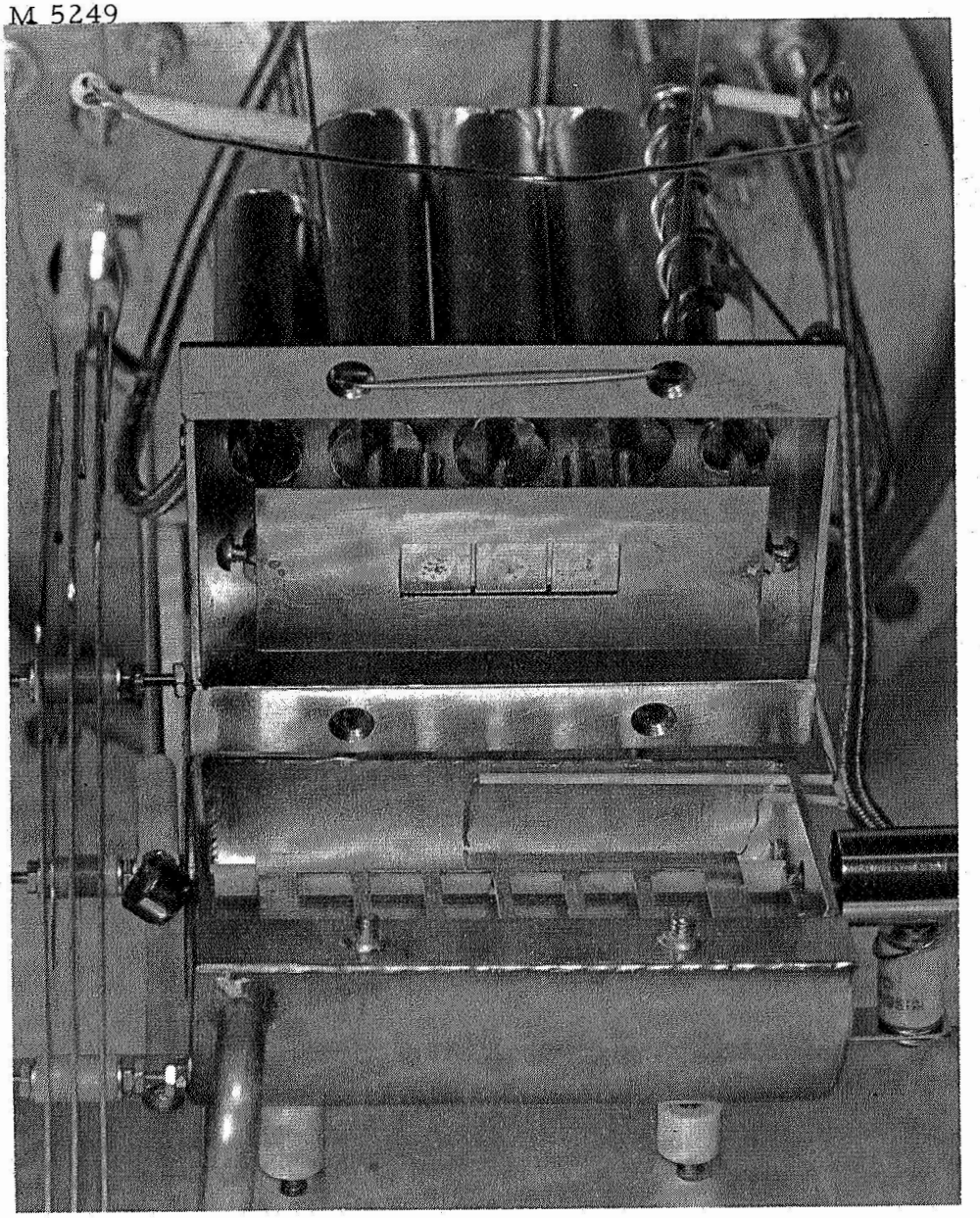

Fig. 11. Interior view of the charge exchange chamber.

M 5266

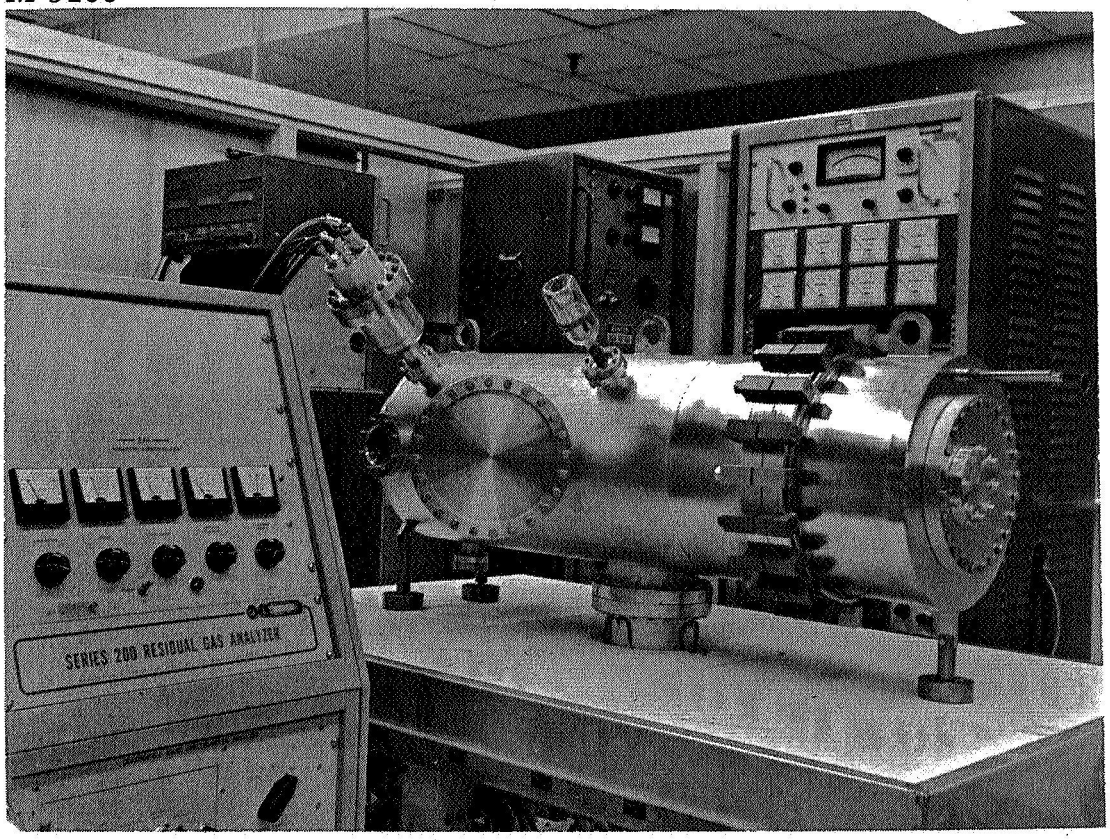

Fig. 12. Vacuum chamber; the quadrupole mass spectrometer is shown in the left foreground and the charge exchange electronics console is in the background.

M 5265

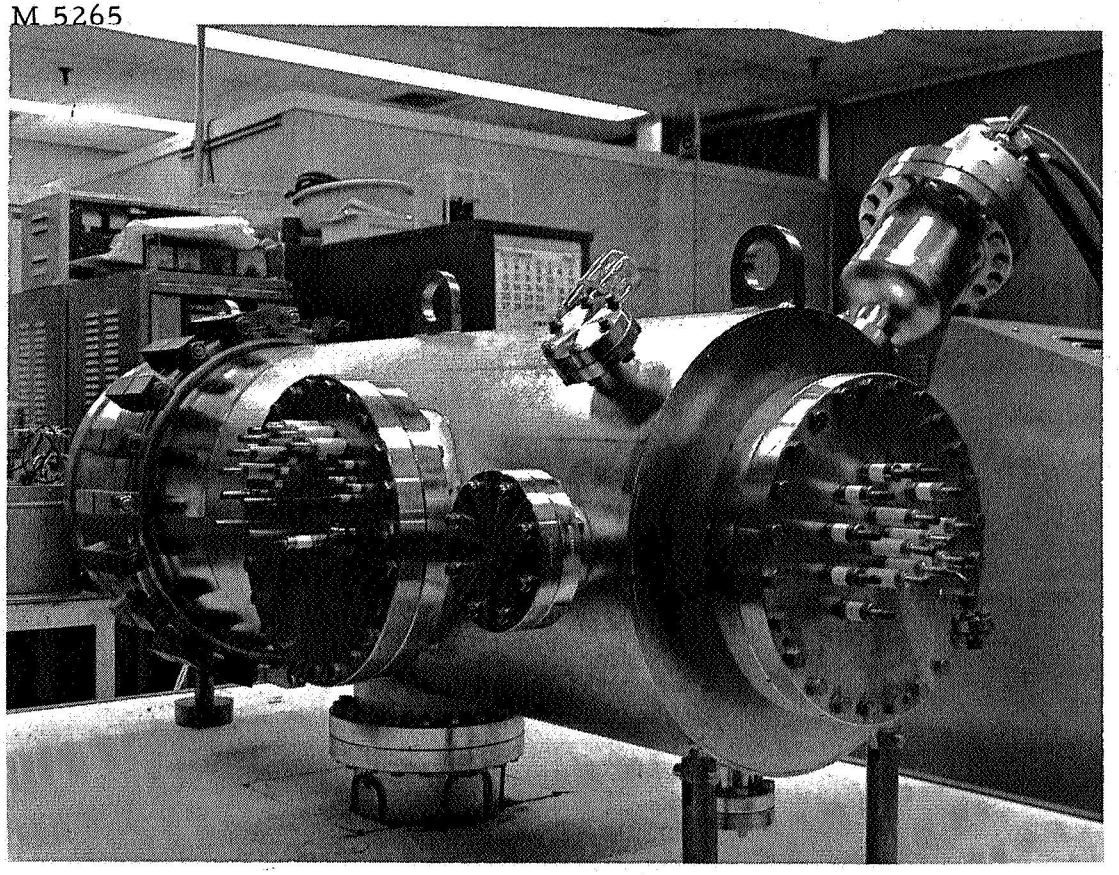

Fig. 13. Vacuum chamber — ion source is mounted on flange at right, charge exchange chamber on flange at left.

The residual gases in the system were analyzed by an EAI quadrupole mass analyzer which has a N_2 sensitivity of 2×10^{-14} Torr and a mass range of 2 to 500 AMU. The total pressure was measured with a Nottingham modified Bayard Alpert ionization gauge tube. This unit has two independent filaments, making possible flash filament measurements. This method of determining the monolayer adsorption time provides an accurate measure of the total residual gas pressure in the 10^{-9} to 10^{-10} Torr range.

The apparatus was placed in the vacuum system and the unit was evacuated under a 250°C bakeout for a 72 hour period. A vacuum of 1.0×10^{-10} Torr was achieved four days after termination of the bakeout. The only residual gases observed by the mass spectrometer are listed in Table III.

TABLE III

Residual Gases Observed by Mass Spectrometer

AMU	Probable Species	Peak Height (in mV Signal)
12	C^+	5
14	CH_2^+, CO^{++}, N_2^+	2
15	CH_3^+	2
16	CH_4^+, O^+	6
17	OH^+	5
18	H_2O^+	12
26	$C_2H_2^+$	5
27	$C_2H_3^+$	5
28	$C_2H_4^+$, CO^+, N_2^+	27
29	$C_2H_5^+$	2
40	Ar^+	7
44	CO_2^+	13

The predominant gases are CO, CO_2, and H_2O. The monolayer coverage time, determined by the flash filament technique, was greater than 8 hours, corroborating the ion gauge reading.

The mercury was loaded into the charge exchange chamber in the following manner. A 10 g charge of triple distilled 99.999% pure mercury was loaded into a 0.45 cm diameter, 7 cm long stainless steel tube (which is sealed at one end). The vacuum system was pressurized to about 1.2 atm with dry nitrogen gas. A vacuum port was unsealed and the mercury quickly transferred into the chamber. The positive pressure prevents the introduction of contaminant gases to the system. The system was re-evacuated to a pressure of 2.3×10^{-8} Torr, which was essentially all mercury vapor. The cesium was loaded in a similar manner. In this case the 99.99% pure cesium metal was loaded in a dry argon environment and frozen in the loading tube. The loading tube filled with the solid cesium was transferred under an inert gas environment, and the system was re-sealed and re-evacuated. This permitted the transfer of cesium without an oil protective film or other contaminant film.

B. Operation of the Equipment

The experimental data consisted of the attenuated ion beam current measured at the Faraday collector I_F and the charge transfer ion currents to the collector electrodes I_A, I_B, and I_C. The guard electrode current I_G was also measured. These were measured as functions of the ion beam energy V, the neutral gas density in the charge transfer chamber (expressed in terms of source temperature T), and the path length L, which is determined by the particular collector.

Before the data were collected, a number of experiments were made in order to establish the necessary experimental conditions. These included measurements made at constant V and T to determine whether variation of the operating parameters of the ion source would have any noticeable effect on the cross section. The mercury vapor flow through

the ion source was varied by changing the temperature of the external mercury reservoir by 15 to 20°K. The ion source was operated at 40 to 180 gauss magnetic fields for dense plasmas and 40 to 70 gauss (where cutoff appeared to occur) magnetic fields for dilute plasmas. The anode (discharge) potential was varied from 35 to 45 V for mercury and the discharge currents ranged from normal operating values of 50 to 100 mA to a high value of 750 mA. None of the variables appeared to affect the magnitude of the measured charge exchange.

All data used in determining the cross section were obtained at constant ion source conditions and constant temperature of the charge exchange source. The ion energy was varied. The approximate ion source operating conditions were a 40 V discharge of about 100 mA, a 50 gauss magnetic field, and a low mercury flow rate through the ion source (dilute plasma operation). The Faraday collector was operated at a small positive bias to insure that secondary electrons did not escape. The collector and the guard electrodes were held to within 0.01 or 0.03 V of each other by operating the electrometers on the ranges which gave either a 0.01 or a 0.03 V drop in the meter.

The charge transfer ion currents were measured at ground potential. The lower electrode was biased by means of batteries and a 10 turn potentiometer to provide an electrostatic field which drives the slow ions to the collector. Preliminary tests were made under three sets of conditions: (a) collector and guard electrodes biased and the lower electrode grounded, (b) collector and guard electrode at a negative bias equal to positive bias on lower electrode, and (c) collector and guard electrodes at ground and lower electrode biased. The results were identical, so that the third method was used to collect the data.

An X-Y recorder was used to plot an electrometer output (I_A, I_B, I_C, or I_F) as a function of the diode potential. The circuit is shown in Fig. 14, and a characteristic plot is shown in Fig. 15. The value of the charge transfer ion current at zero field was obtained by extrapolating the linear portion of the positive bias current to zero bias. For ion energies above

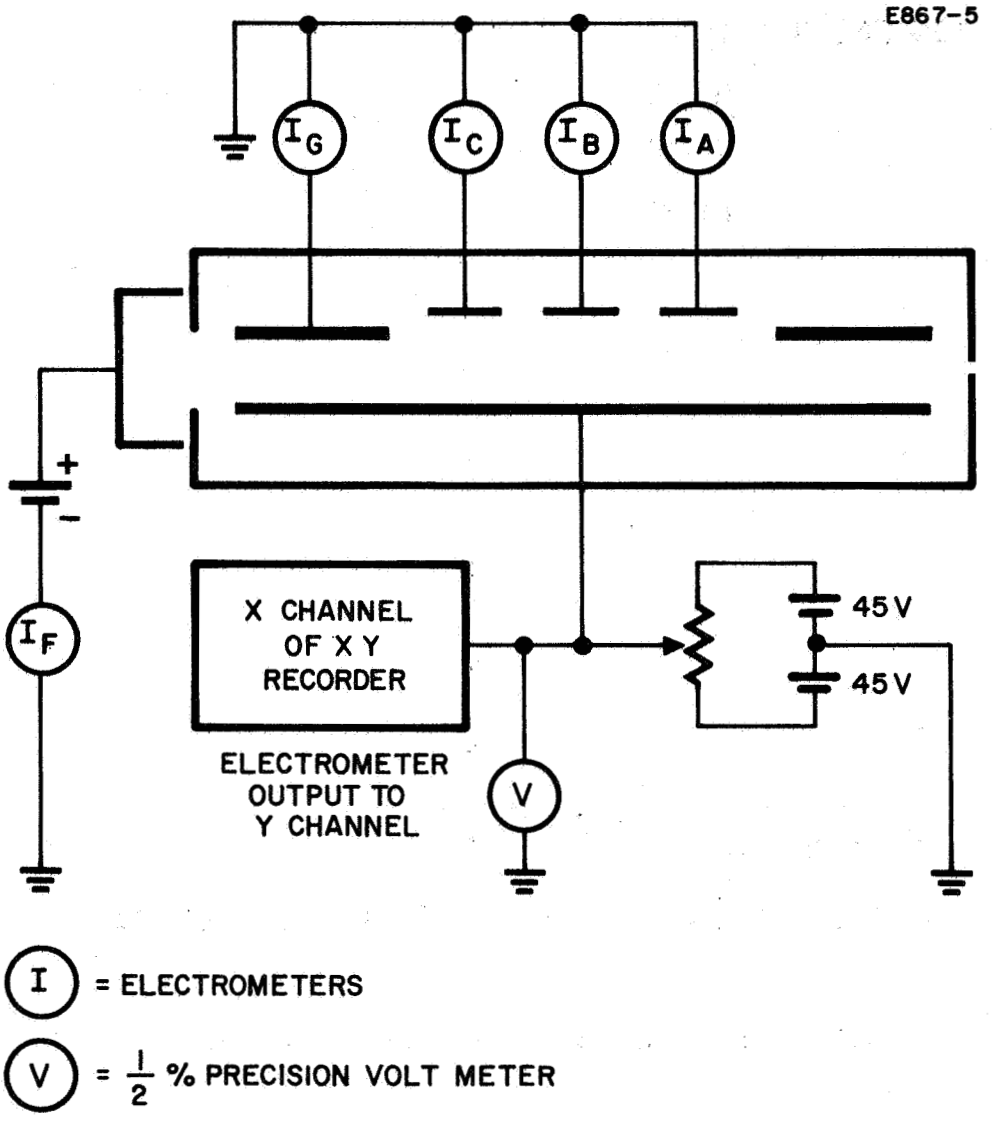

Fig. 14. Schematic representation of the electrical circuits of the charge transfer chamber.

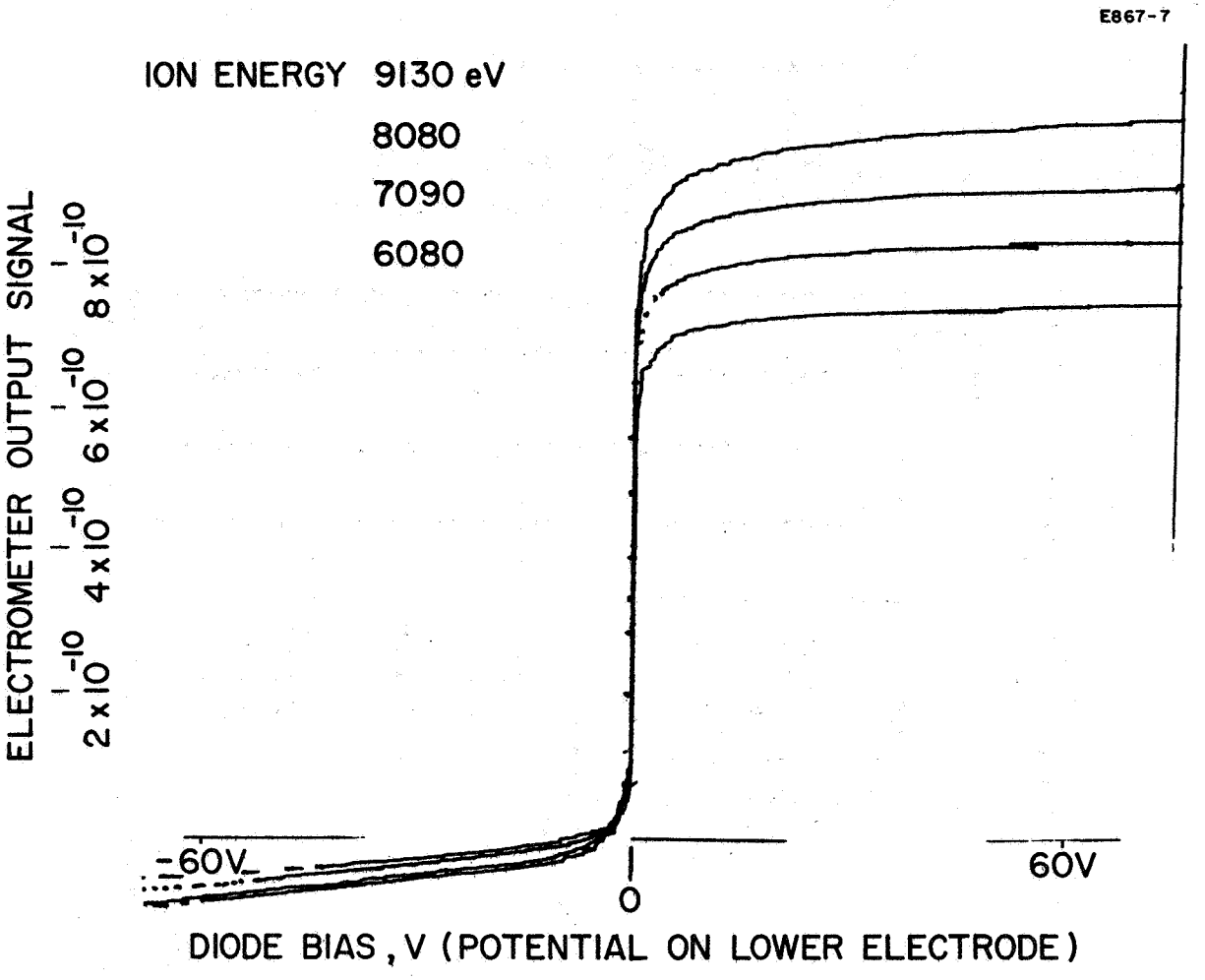

Fig. 15. Collector current as a function of diode bias potential.

approximately 5 kV, a small fraction of the slow ion current results from the ionization reaction (No. 4 of Table I). The magnitude of the slow ions due to this reaction is determined by measuring the electron current which is equal in value. This was accomplished by extrapolating the linear portion of the negative bias current to zero bias. This value is subtracted from the positive ion current to obtain the charge exchange ion current. Extrapolation of the negative bias currents to zero bias also takes care of any secondary electron component in the collector currents, which could have represented a source of error.

The experiments were conducted in vacuum system pressures of 6×10^{-9} to 1.1×10^{-7} Torr. Mass spectrometer analysis showed that the residual gas is predominately mercury vapor. This was confirmed by the fact that the observed pressures varied directly with the operating temperature of the charge transfer chamber. Similar situations exist for the cesium case.

IV. RESULTS

A. Calculation of Cross Section

Charge exchange data were obtained for mercury ions of 115 to 10400 eV energy. Essentially all the data were obtained for mercury vapor source temperatures ranging from 256.56 to 277.78°K, which correspond to mercury vapor pressures of 3.35×10^{-5} to 3.26×10^{-4} Torr. A few data points were obtained for source temperatures up to 290.85°K (vapor pressure of 1.15×10^{-3} Torr). The cesium data were obtained for ions of 500 to 5000 eV energy. The vapor source temperature ranged from 314.91 to 322.76°K, which corresponds to vapor pressures of 7.05×10^{-6} to 1.40×10^{-5} Torr.

The selection of the vapor pressure versus temperature relationship is of critical importance because of the significant differences that exist between many of these expressions. The extensive literature on mercury vapor pressure measurements was reviewed by Ditchburn and Gilmour.[22] They analyzed data and obtained the expression

$$\log P = 10.3735 - \frac{3308}{T} - 0.8 \log T.$$

Dauphinee[23] experimentally verified this at low pressures. Busey and Giaugue[24] reviewed the previous experiments and presented a tabular summary which is essentially identical with the values obtained from Ditchburn's[22] equation. These papers[22-24] (especially 24) are cited in the most recent thermochemical tables and were used in this experiment. The cesium vapor pressures were obtained from Taylor and Langmuir's[25] expression

$$\log P = 11.0531 - 1.35 \log T - \frac{4041}{T} \quad (\text{for } T > 302^{\circ}\text{K}) .$$

It is important to note that the vapor pressure expressions presented in several popular handbooks are significantly different from the above.

The charge transfer cross section σ was calculated from the attenuated ion beam current measured at the Faraday collector I_F, the slow ion current I_C to some collector "C," the length L of "C" (which is the charge exchange region), the distance D from the end of "C" to the end of the guard electrode, the vapor source temperature T, and the vapor pressure P at this temperature. A digital computer was used to obtain σ by successive approximations.

The exact expression for σ is

$$I = I_o \exp^{-\sigma n L} \tag{7}$$

where I_o is the ion beam entering the charge transfer region of length L, with an atom density n in the beam path. The attenuated ion beam I leaves this region. For monatomic gases such as mercury and cesium, it is possible to state the number density as $n = (N/V) = P/RT$. Solving for σ, we obtain

$$\sigma = \ln\left(\frac{I_o}{I}\right) \frac{RT}{PL} \quad . \tag{8}$$

A trial value of σ was obtained by approximating the value of I_o by $(I_F + I_C)$ and the value of I by I_F

$$\sigma = \ln\left(\frac{I_F + I_C}{I_F}\right) \frac{RT}{PL} \quad . \tag{9}$$

This value of σ was used to determine the magnitude of the ion beam at a point D cm from the point at which I_F is measured

$$I_{F_o} = I_F \exp \sigma \frac{PD}{RT} \quad . \tag{10}$$

This value I_{F_o} represents an approximation of the attenuated beam which leaves the collector "C" region, and is used to obtain a better value of the cross section σ_o:

$$\sigma_o = \ln\left(\frac{I_{F_o} + I_c}{I_{F_o}}\right)\frac{RT}{P}\,\frac{1}{L} \quad . \tag{11}$$

If

$$1 - \frac{\sigma_o}{\sigma} < 10^{-4} \quad ,$$

the values are converged and the calculation is complete. If this condition does not apply σ_o is substituted for σ in (10) and a new cycle is performed. In practice, only two or three cycles were necessary for convergence.

A total of 1023 mercury data points were obtained by this method. Of this total, the majority (62%) were obtained for mercury ions of 1000 to 5000 eV energy, 26% for higher energy ions and 12% for lower energy ions. All of the values are plotted in Fig. 16. The most extensive set of data was obtained at a mercury vapor pressure of 1.65×10^{-5} Torr. These data are presented in Fig. 17.

A least squares calculation was made and the results are as follows: $\sigma^{1/2} \times 10^8 = 8.623 - 0.6354 \log V$. This line is shown in Fig. 16 and 17. The mean deviation in $\sigma^{1/2}$ is 0.157 and the standard deviation is 0.195. The latter corresponds to 3% of $\sigma^{1/2}$ and about 6% of σ. The bar on the right hand end of the line in Figs. 16 and 17 indicates the magnitude of the standard deviation. The $\sigma^{1/2}$ line is shown in Fig. 18 for comparison with previous values.

When the mercury charge exchange measurements were completed, the system was cleaned and the cesium ion-atom charge exchange cross-section was measured to correlate this study with previous cesium studies.

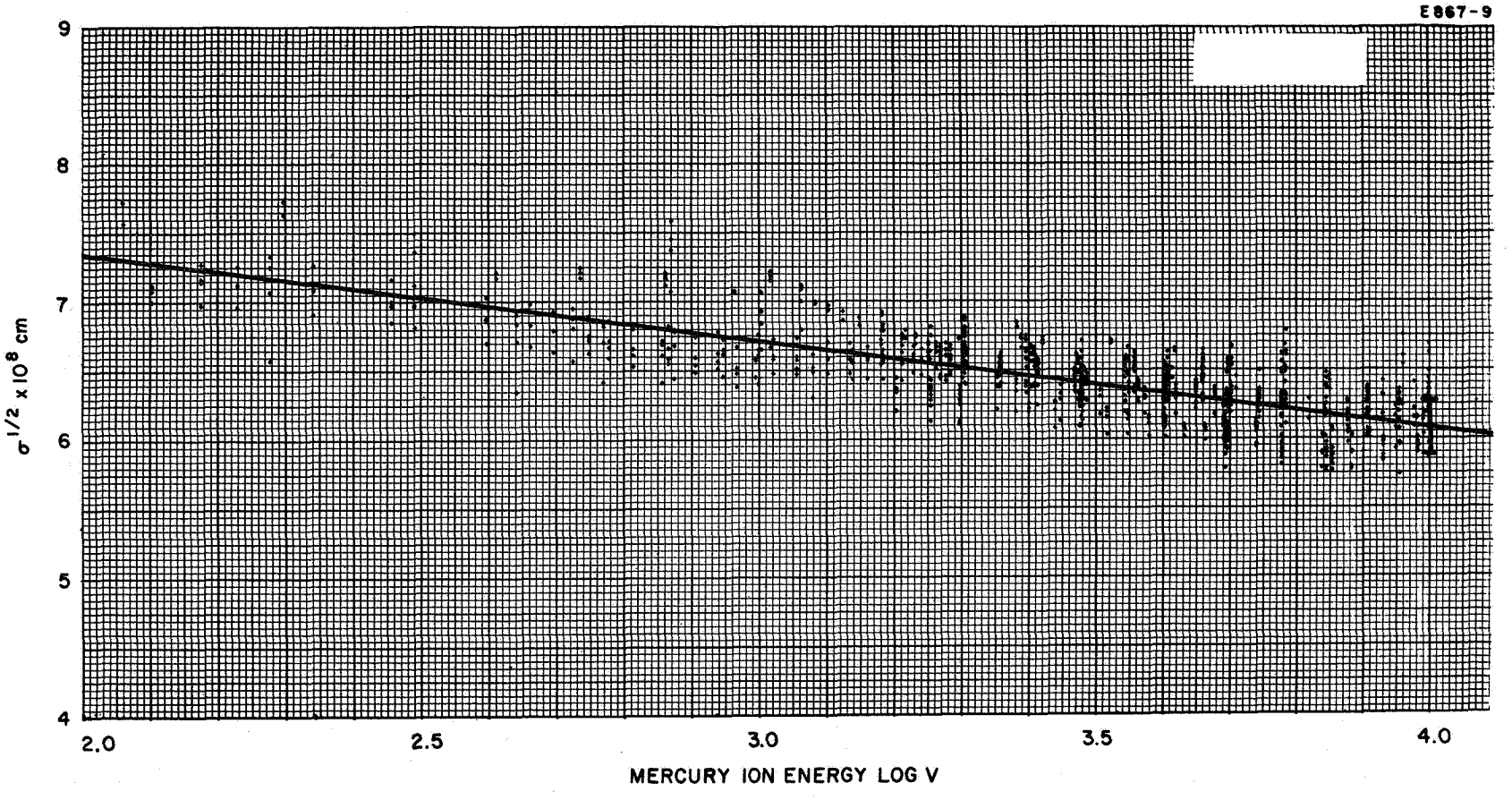

Fig. 16. Complete plot of the 1023 mercury charge exchange cross section values.

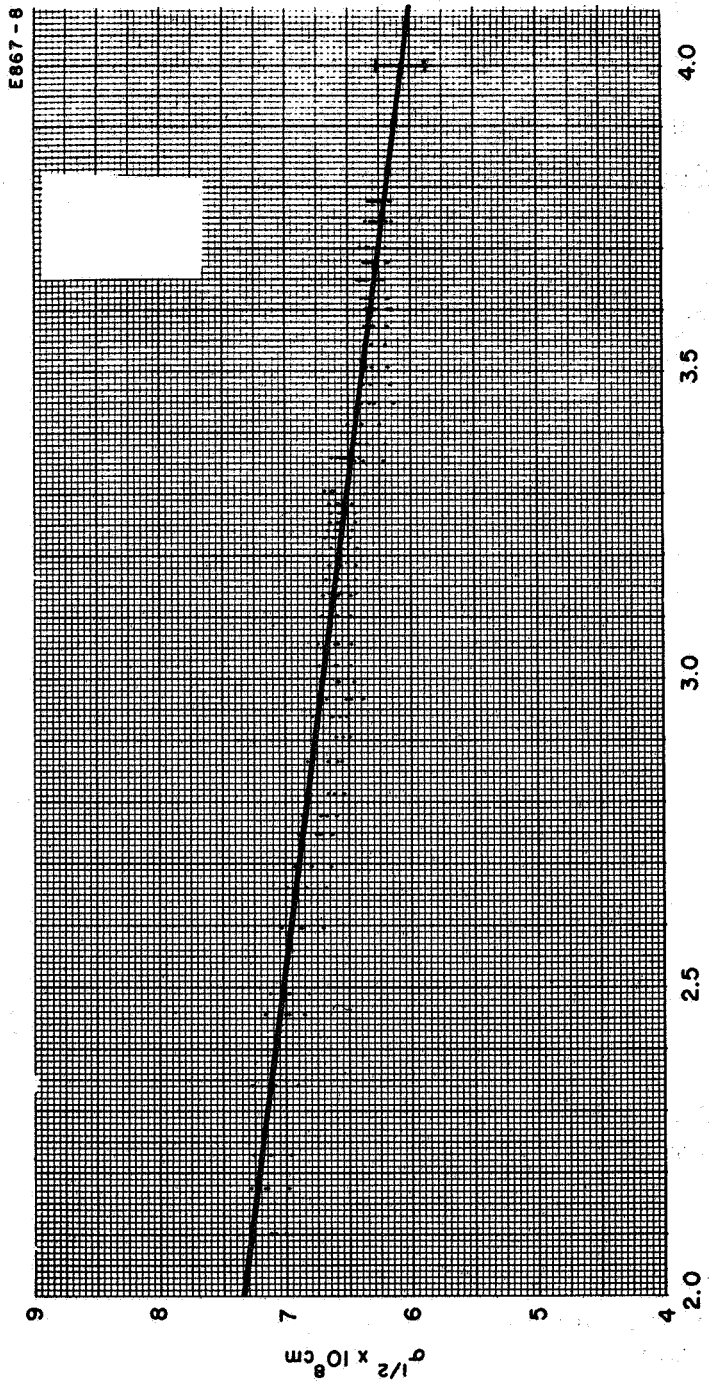

Fig. 17. Plot of mercury charge exchange cross section values for mercury vapor pressure of 1.65×10^{-5} Torr.

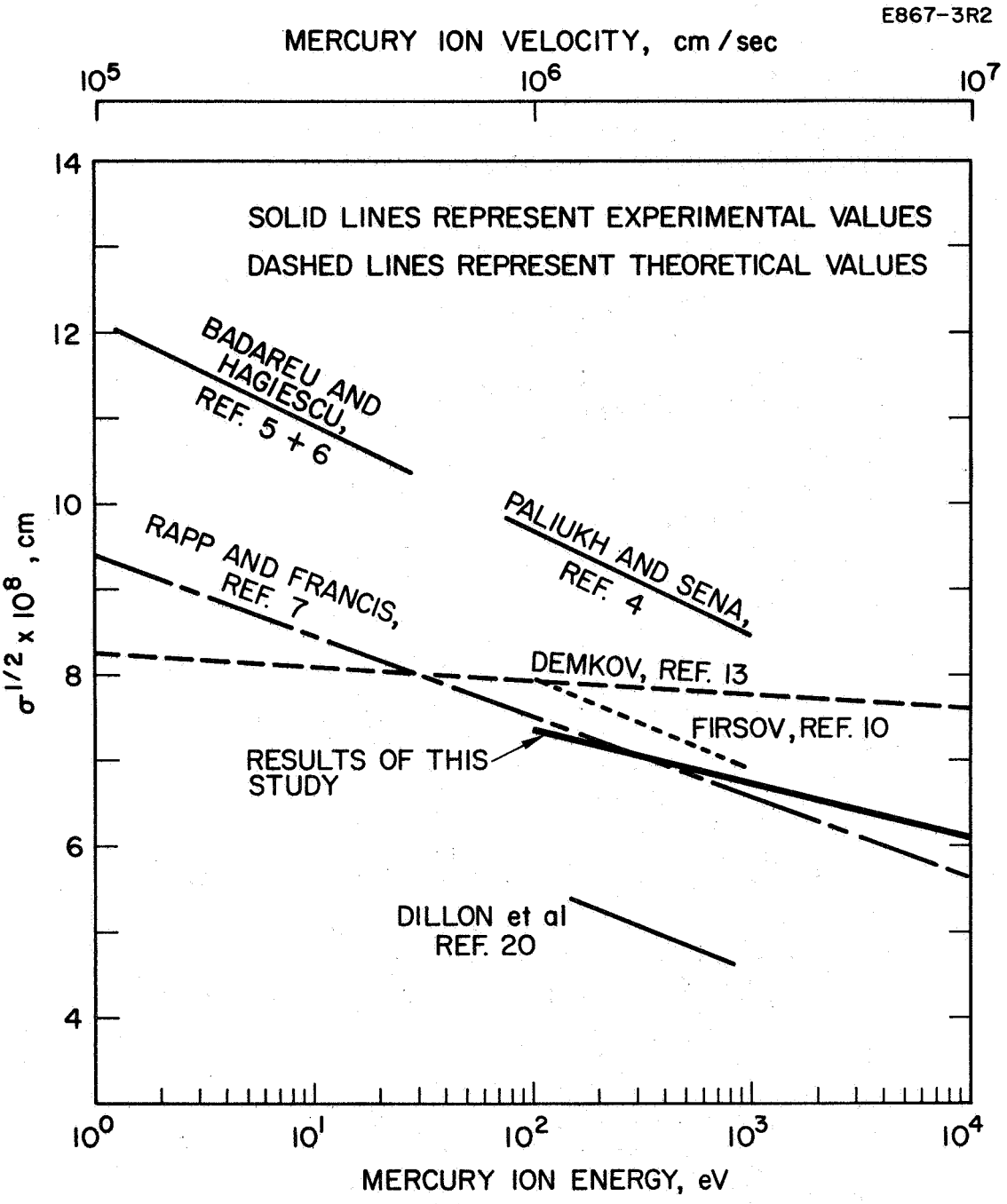

Fig. 18. Experimental and theoretical mercury charge exchange cross sections.

Approximately 100 data points were obtained in the ion energy range of 500 to 5000 eV. The values were slightly greater than those reported by Perel, et al.,[3] and were clustered about the values reported by Marino.[1,2] These are shown in Fig. 19. No attempt was made to fit these data to Marino's[2] expression (eq. 6) which describes the oscillations in the cross section.

B. Error Analysis

There are two general sources of error which may be present in the charge exchange cross section. There is a random error which may result from uncertainty in the determination of such experimental parameters as the primary and the charge exchange ion currents, the vapor temperature and pressure, and the linear dimensions of the interaction region. This is the error which is associated with the random deviation about a mean value. The second source of error is the systematic (or nonrandom) error in which the experimentally determined value of σ has a specific factor which results from a nonrandom error. Examples of these source include the presence of doubly charged ions in the primary ion beam and an uncertainty in the ion energy in the primary ion beam.

The random error in the calculated value of the charge transfer cross section was estimated based on the following estimates of uncertainty in the data. The ion currents were assigned a 3% uncertainty which was based on the calibration certification of the electrometers. A $\pm 0.05^{\circ}K$ error was assigned to the temperature. This value was obtained from the calibration of the potentiometer bridge. Ditchburn[22] assigned a probable accuracy of 2% for the vapor pressure-temperature relationship for mercury. The collectors were machined and assembled to an accuracy of ± 0.003 cm.

The total random error in the cross section was obtained by taking the derivative of σ with respect to each of these quantities. The total random error was calculated to be $\pm 5.5\%$. The major

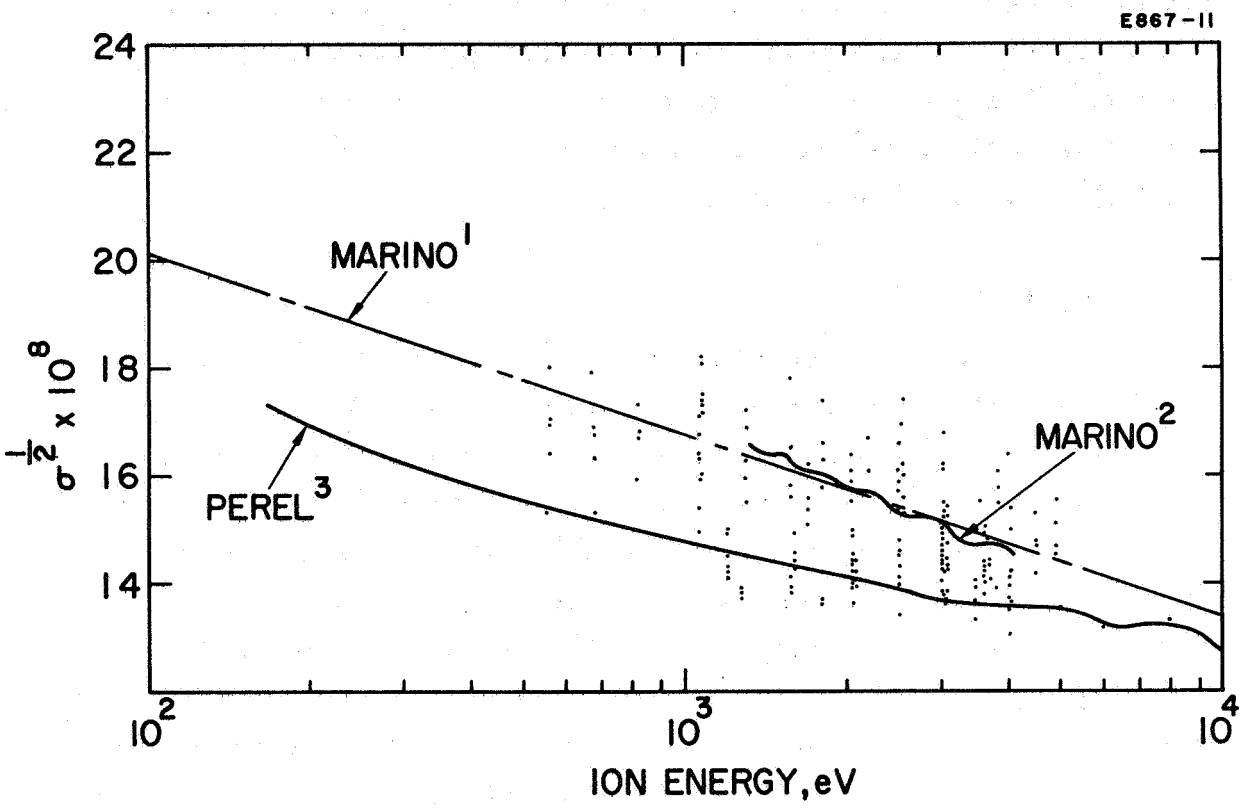

Fig. 19. Cesium charge exchange cross sections.

components were the uncertainty in the collector current I_c which gave a ±3% error and the uncertainty in the vapor pressure which represented a ±2% error. This value is in very good agreement with the 6% value of the standard deviation, indicating that the analysis of the total random error is based on reasonable estimates of the individual uncertainties.

The presence of doubly charged mercury ions in the ion beam could affect the value of σ in two ways. First, the true ion current would be smaller than the observed ion current I_F, causing the true cross section to be larger than the apparent one. The second effect is that the reaction $Hg^{++} + Hg^{o} \rightarrow Hg^{+} + Hg^{+}$ ($_{20}\sigma_{11}$) is not a resonant one; therefore, $_{20}\sigma_{11}$ should be much smaller than $_{10}\sigma_{01}$. Based on experimental studies made by Milder[26] and King,[27] the Hg^{++} content of the ion beam may be as large as 2.5% of the Hg^{+} ion current for a 40 V discharge potential. If it is assumed that the maximum Hg^{++} value is 2.5% of the beam, the maximum error in I_F would be 5%, based on an assumption of the worst case when $_{20}\sigma_{11} << {}_{10}\sigma_{01}$. Under this condition the true cross section would have been 5% greater than the observed value. The following experimental observation indicates that the probable value of this systematic error is much smaller than 5%.

During the preliminary survey studies the discharge voltage was varied from 35 to 45 V. Based on King's report,[27] the Hg^{++} current should have varied from 1 to 4% of the beam. There was no noticeable effect on the observed cross section, indicating that the Hg^{++} current from the low pressure-low voltage ion source was not large enough to affect the results.

Care was taken to prevent an error caused by secondary electron emission currents. The Faraday collector was sufficiently deep and operated at a positive potential to prevent the loss of secondary electrons. The charge transfer ions were collected at low diode voltages (about 0.5 to 45 V) and the ion currents were extrapolated to zero bias, thus minimizing any secondary electron currents.

A small systematic error may exist in the determination of the ion energy from the screen electrode potential. In operation, the ions are formed in the source at some potential between the anode potential and the screen-cathode potential. The ions then drift to the screen, where they are extracted. In the worst case, the mercury ions are assumed to have been formed at the anode potential and thus the true ion energy would be 40 V larger than that given by the screen electrode potential. This would represent a 4% error for 100 V ions, a 0.5% error for 1000 V ions, and a 0.07% error for 10,000 V ions. Because the greatest part of the data was obtained above 1000 V, this factor is negligible.

C. Discussion of Results

The experimental results of the mercury charge transfer cross section measurements obtained in this program are significantly smaller than those reported by Paliukh and Sena[4] and Badareu and Hagiescu.[5, 6] This is shown in Fig. 18.

Puliukh and Sena's value of the cross section for 990 eV ions (the highest energy reported in their work) is 61% larger than the value obtained in the present study. This difference could be the result of an error of less than 5°K in the determination of the vapor temperature. There is a fair probability that the temperature could have been underestimated in the previous experiments, because both were conducted in glass tubes using a glow discharge as a source of ions. The low thermal conductivity of the glass could result in small temperature differentials in the apparatus.

The much smaller values reported by Dillon, et al.,[20] must have resulted because they used a single argon value to standardize the apparatus to give similar results to a previous experiment.

The experimental results obtained in this work are in good agreement with the theoretical values of Rapp and Francis[7] and are lower than the theoretical values obtained from Demkov's expression[13] and from Firsov.[10] These are shown in Fig. 18.

The data were analyzed to determine whether oscillations in σ (such as those observed by Perel[3] and Marino[2] in the cesium case) were present in the mercury case. Within the accuracy of the error limits (approximately 5%), there was no evidence of any periodic fluctuations.

V. CONCLUSIONS

The resonant charge exchange cross section for singly charged mercury ions and mercury atoms has been measured over a two decade range in ion energy and neutral gas density with a probable accuracy of about 5%. In contrast to previous mercury experiments, considerable attention was given to the design of the apparatus and the determination of operating conditions in order to measure the resonant reaction between ground state ions and ground state atoms. In addition, the same apparatus was used to measure the charge transfer cross section of cesium ions and atoms, in order to correlate the two cases and thus verify the mercury experiment.

These results are very important to the development of ion thrusters because the formation of unfocused ions by charge exchange results in the erosion of critical components such as the accelerator electrode and the neutralizer. Knowledge of the charge exchange cross section is important to the design of the ion thrusters and the evaluation of laboratory life test data. The values obtained in this study are significantly smaller than the values which have been used previously in the prediction of electrode erosion rates.

REFERENCES

1. L.L. Marino, A.C.H. Smith, and E. Caplinger, Phys. Rev. 128, 2243 (1962).

2. L.L. Marino, Phys. Rev. 152, 46 (1966).

3. J. Perel, R.H. Vernon, and H.L. Daley, Phys. Rev. 138, A937 (1965).

4. B.M. Paliukh and L.A. Sena, Zh. Eksperim. i Teor. Fiz, 20, 481 (1950). SLA Translation Center 60-18509.

5. E. Badareu and M. Hagiescu-Miriste, Acad. Rep. Populare Romine, Bul. Stiint Sect. Stiinte Mat. Fiz. 2, 603 (1950).

6. E. Badareu, M. Hagiescu-Miriste, Acad. Rep. Populare Romine, Studii Cercetari Fiz. 10, 429 (1959).

7. D. Rapp and W.E. Francis, J. Chem. Phys. 37, 2631 (1962).

8. J.B. Hastead, Advan. in Electron. and Electron Physics 13, 1 (1960); also in Atomic and Molecular Processes, D.R. Bates, Ed. (Academic Press, New York, 1962). See also J.B. Hastead, Physics of Atomic Collisions (Butterworth's, London, 1964).

9. H.S.W. Massey and R.A. Smith, Proc. Roy. Soc. (London), Ser. A 142, 142 (1933).

10. O.B. Firsov, Zh. Eksperim. i Teor. Fiz. 21, 1001 (1951); Tech. Transl. R671.

11. B.M. Smirnov, Zh. Eksperim. i Teor. Fiz. 46, 1017 (1964); Soviet Phys.-JETP 19, 692 (1964).

12. B.M. Smirnov, Zh. Eksperim. i. Teor. Fiz. 47, 518 (1964); Soviet Phys.-JETP 20, 345 (1965).

13. Yu. N. Demkov, Uch. Zap. Leningr. Gos. 146, 74 (1952); Translation NHSA TTF9707.

14. F.J. Smith, Phys. Letters 20, 271 (1966).

15. H. Mayer, Z. Physik 67, 240 (1931); [Chem. Abstract 25, 4158^5 (1931)].

16. R.M. Kushnir, B.M. Paliukh, and L. A. Sena, Bull., Acad. Sci. USSR, Phys. Ser. (English Transl.) 23 995 (1959).

17. I. Popescu, Acad. Rep. Populare Romine, Rev. Phys. 2, 199 (1959).

18. I. Popescu Iovitsu and N. Ionescu Pallas, Soviet Phys.-Tech. Phys. 4, 781 (1960).

19. I. Popescu Iovitzu and N.J. Ionescu Pallas, Proc. Phys. Soc. (London) 75, 807 (1960).

20. J.A. Dillon, Jr., W.F. Sheridan, H.D. Edwards, and S.N. Gnosh, J. Chem. Phys. 23, 776 (1955).

21. J.B. Hastead, Proc. Roy. Soc. (London), Ser. A205, 421 (1951).

22. R.W. Ditchburn and J.C. Gilmour, Rev. Mod. Phys. 13, 310 (1941).

23. T.M. Dauphinee, J. Chem. Phys. 19, 389 (1951).

24. R.H. Busey and W.F. Giaugue, J. Am. Chem. Soc. 75, 806 (1953).

25. J.B. Taylor and I. Langmuir, Phys. Rev. 51, 753 (1937).

26. M.L. Milder, NASA TN D-1219, July 1962.

27. H.J. King, Final Report, Contract NAS 8-1684, January 1963.

DISTRIBUTION LIST

Addressee	Number of Copies
National Aeronautics & Space Administration Washington, D. C. 20546 Attention: RNT/James Lazar	2
National Aeronautics & Space Administration Lewis Research Center 21000 Brookpark Road Cleveland, Ohio 44135	
Attention: Spacecraft Technology Procurement Section, MS 54-2	1
Technology Utilization Office, MS 3-19	1
Technical Information Div., MS 5-5	1
Library, MS 60-3	2
Spacecraft Technology Division, MS 54-1	
C. C. Conger	1
E. Otto	1
H. R. Hunczak	1
R. R. Nicholls	6
R. Rulis	1
S. Jones	2
Electric Propulsion Lab., MS 301-1	
W. Moeckel	1
H. R. Kaufman	1
E. A. Richley	2
J. Ferrante	3
Report Control Office, MS 5-5	1
National Aeronautics & Space Administration Scientific and Technical Information Facility P. O. Box 33 College Park, Maryland 20740 Attention: NASA Representative RQT-2448	6
National Aeronautics & Space Administration Marshall Space Flight Center Huntsville, Alabama 35812	
Attention: Ernest Stuhlinger (M-RP-DIR)	1
I. Dalins	1
Research and Technology Division Wright-Patterson AFB, Ohio 45433 Attention: AFAPL (APIE-2)/R. F. Cooper	1

Addressee	Number of Copies
AFWL Kirtland AFB, New Mexico 87417 Attention: WLPC/Capt. C. F. Ellis	1
Aerospace Corporation P. O. Box 95085 Los Angeles, California 90045 Attention: Library/Technical Documents Group	1
Jet Propulsion Laboratory 4800 Oak Grove Drive Pasadena, California 91103 Attention: J. W. Stearns D. Kerrisk	1 1
Electro-Optical Systems, Inc. 300 North Halstead Pasadena, California 91107 Attention: R. C. Speiser	2
TRW Inc. TRW Systems Group One Space Park Redondo Beach, California 90278 Attention: D. B. Langmuir E. Cohen D. Goldin	1 1 1
Westinghouse Astronuclear Laboratories Electric Propulsion Laboratory Pittsburgh, Pennsylvania 15234	1
General Electric Space Flight Propulsion Laboratory Cincinnati, Ohio 45215 Attention: M. L. Bromberg	1
Litton Precision Products Surface Physics Department Minneapolis, Minnesota Attention: G. K. Wehner	1
Varian Associates 611 Hansen Way Palo Alto, California 94304 Attention: Technical Library	1

Addressee	Number of Copies
National Aeronautics & Space Administration Ames Research Center Moffett Field, California 94035 Attention: Library	1
University of California Space Science Laboratory Berkeley, California 94720 Attention: H. P. Smith	1
United Aircraft Corporation Research Laboratories East Hartford, Connecticut 06108 Attention: R. G. Meyerand, Jr.	1
National Aeronautics & Space Administration Langley Research Center Langley Field Station Hampton, Virginia 23365 Attention: Technical Library	1
Colorado State University Fort Collins, Colorado 80521 Attention: L. Baldwin W. Mickelsen	1 1
U. S. Atomic Energy Commission P. O. Box 62 Oak Ridge, Tennessee 37831 Attention: Technical Information Service Ext.	1
Republic Aviation Corporation Plasma Propulsion Laboratory Farmingdale, Long Island, New York 11735 Attention: A. Kunen	1
United States Air Force Office of Scientific Research Washington, D. C. 20025 Attention: M. Slawsky	1
Naval Research Laboratory Washington, D. C. 20025 Attention: A. C. Kolb	1

Addressee	Number of Copies
Case Institute of Technology 10900 Euclid Avenue Cleveland, Ohio 44106 Attention: Professor Eli Reshotko	1
Litton Systems, Inc. Beverly Hills, California 90213 Attention: A. S. Penfold	1
General Electric Company Missile and Space Division Space Sciences Laboratory P. O. Box 8555 Philadelphia, Pennsylvania 19101 Attention: P. Gloevsen	1
University of California Laurence Radiation Laboratory Livermore, California Attention: S. A. Colgate	1
Rome Air Development Center Headquarters Air Force Systems Command Griffiss AFB, New York 13442 Attention: RALRP	1
Swiss Federal Institute of Technology Zurich, Switzerland Attention: Library	1
J. T. Kotnik 16808 Westdale Avenue Cleveland, Ohio 44135	1
Cornell Aeronautics Labs. Buffalo, New York 14221 Attention: D. Lockwood	1
National Aeronautics & Space Administration Goddard Space Flight Center Greenbelt, Maryland 20771 Attention: William Isley, Code 734	1
Wright-Patterson AFB Dayton, Ohio 45433 Attention: AFADL (API) G. Sherman FDCL Paul Polishuk	1 1